

Exotic Leptons: Higgs, Flavor and Collider PhenomenologyWolfgang Altmannshofer,¹ Martin Bauer,^{1,2} and Marcela Carena^{1,2,3}¹*Fermi National Accelerator Laboratory, P.O. Box 500, Batavia, IL 60510, USA*²*Enrico Fermi Institute, University of Chicago, Chicago, IL 60637, USA*³*Kavli Institute for Cosmological Physics,
University of Chicago, Chicago, IL 60637, USA*

We study extensions of the standard model by one generation of vector-like leptons with non-standard hypercharges, which allow for a sizable modification of the $h \rightarrow \gamma\gamma$ decay rate for new lepton masses in the 300 GeV - 1 TeV range. We analyze vacuum stability implications for different hypercharges. Effects in $h \rightarrow Z\gamma$ are typically much smaller than in $h \rightarrow \gamma\gamma$, but distinct among the considered hypercharge assignments. Non-standard hypercharges constrain or entirely forbid possible mixing operators with standard model leptons. As a consequence, the leading contributions to the experimentally strongly constrained electric dipole moments of standard model fermions are only generated at the two loop level by the new CP violating sources of the considered setups. We derive the bounds from dipole moments, electro-weak precision observables and lepton flavor violating processes, and discuss their implications. Finally, we examine the production and decay channels of the vector-like leptons at the LHC, and find that signatures with multiple light leptons or taus are already probing interesting regions of parameter space.

I. INTRODUCTION

In 2012, the Large Hadron Collider (LHC) experiments ATLAS and CMS both reported the discovery of a Higgs-like boson at $m_h \simeq 125$ GeV [1, 2]. At this mass, many of its Standard Model (SM) couplings are experimentally accessible, which makes the question whether new physics manifests itself through modifications of these couplings one of the most interesting ones for the LHC to answer. The hints for a possible enhancement of the Higgs to diphoton decay rate [3–6] therefore triggered a lot of activity in the model building community (see e.g. [7–37]). In the latest analysis by ATLAS [38], this excess of events in the $h \rightarrow \gamma\gamma$ channel leads to a best fit value of the signal strength of $1.65 \pm 0.24^{+0.25}_{-0.18}$ times the predicted SM value, while with the full 7+8 TeV data set, the CMS $h \rightarrow \gamma\gamma$ signal has gone down to $0.78^{+0.28}_{-0.26}$ [39]. The $h \rightarrow \gamma\gamma$ decay is loop induced in the SM and therefore highly sensitive to new physics effects. It will be extremely interesting to monitor if a significant deviation from the SM prediction can be established at the 13 TeV LHC run. Although all other presently measured decay rates are compatible with the SM predictions, there is still room to consider NP effects, and it is also interesting to explore connections with modifications in these channels. Here we concentrate on the properties of models which can lead to a significant modification in $h \rightarrow \gamma\gamma$, without sizable effects in other channels. The properties of such models can be narrowed down considerably [14].

A promising class of models to this end are extensions of the SM by a set of new vector-like leptons, transforming as electro-weak doublets and singlets, respectively. Sizable Yukawa couplings between the Higgs and these new states allow for a modification of the $h \rightarrow \gamma\gamma$ rate without modifying the main production process via gluon fusion. The price for this modification is a severe vacuum instability bound, because the new Yukawa couplings will drive the Higgs quartic coupling negative at a scale around 10 TeV [16, 17, 40]. In addition, possible mixing terms between the new vector-like leptons and the SM leptons can induce 1-loop contributions to electric and magnetic dipole moments (EDM/MDM), as well as tree level contributions to lepton flavor violating processes, which are strongly constrained experimentally [23, 32, 41]. While the vacuum instability bound calls for an extension of this model at a relatively low scale (see e.g. [29, 36, 42]), the latter constraints have been usually avoided in the literature by either assuming very small coefficients for the mixing operators or by invoking a discrete symmetry [16, 17, 22]. In this work, we argue that a different hypercharge assignment to the new vector-like leptons can in principle not only relax the vacuum instability bound, but simultaneously also ensures automatically that the leading contributions to dipole moments only arise at the 2-loop level.

We explore two scenarios: One, in which the hypercharge of the weak doublets of new vector-like leptons is $Y = -3/2$ and one where it is $Y = -5/2$. In Section II, we introduce these models and discuss the masses and couplings of the new leptons. One important difference between the two scenarios is, that the first model allows for a single renormalizable coupling to SM leptons, while in the latter only non-renormalizable operators can couple the vector-like leptons to the SM leptons. In Section III, we discuss the modified Higgs phenomenology of the models. We compute the $h \rightarrow \gamma\gamma$ and $h \rightarrow Z\gamma$ decay rates, which are both affected by the presence of relatively light vector-like leptons. We also discuss the vacuum stability bounds in this setup. In Section IV, we discuss the implications of the new vector leptons for EDMs, MDMs, as well as the S and T parameter. In Section V, Z pole observables and lepton flavor violating processes are used to derive bounds on the model parameters that mix the vector-like leptons with SM leptons. Such constraints are also highly relevant for scenarios in which the new vector leptons share the quantum numbers with the SM leptons. Finally, in Section VI, we discuss the production and decay processes of the new vector leptons. We compute the relevant cross sections of final states with multiple light leptons and taus and confront them with the existing searches at the LHC.

II. MODELS WITH EXOTIC HYPERCHARGES

The loop induced coupling of the Higgs to two photons is sensitive to the Yukawa coupling of any internal fermion and to its electric charge, see the diagram on the left hand side of Figure 1. As is well known [14], the contributions from chiral fermions interfere destructively with the W loop contribution, which dominates in the SM. On the other hand, extensions of the SM with vector-like leptons which couple to the Higgs, can both enhance and suppress the $h \rightarrow \gamma\gamma$ decay rate, because in contrast to chiral leptons, vector-like leptons can interfere also constructively with the W contribution. Colored new matter is additionally constrained by data, because it also affects the gluon fusion production cross section of the Higgs, which in turn leads to modifications of all Higgs signal strengths [7, 9, 14, 25, 26, 28, 43–47].

A sizable correction of the $h \rightarrow \gamma\gamma$ rate due to vector-like leptons, requires large Yukawa couplings of the leptons to the Higgs, which in turn contribute to the beta function of the Higgs quartic coupling via the box diagrams depicted on the right-hand side of Figure 1. This will cause the Higgs quartic coupling to run negative at a very low scale [17]. We argue, that this scale can be in principle considerably higher, if the new vector-like leptons carry larger electric charges. Larger electric charges affect the $h \rightarrow \gamma\gamma$ decay rate, but are not felt by the Higgs quartic coupling at the

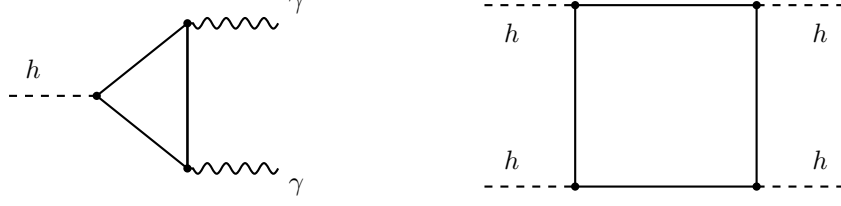


Figure 1. Feynman diagrams involving the new vector-like leptons (straight lines), which are responsible for 1-loop contributions to the $h \rightarrow \gamma\gamma$ decay rate (left) and the running to the Higgs quartic coupling (right).

1-loop level.

Therefore, we study the effects of extending the SM by one generation of new vector leptons, which transform as doublets and singlets under $SU(2)_L \times U(1)_Y$,

$$\begin{aligned}
 L_L &= \begin{pmatrix} N_L \\ E_L \end{pmatrix} = (1, 2)_{-1/2-n} , & \tilde{L}_R &= \begin{pmatrix} \tilde{N}_R \\ \tilde{E}_R \end{pmatrix} = (1, 2)_{-1/2-n} , \\
 \tilde{E}_L &= (1, 1)_{-1-n} , & E_R &= (1, 1)_{-1-n} .
 \end{aligned} \tag{1}$$

The case $n = 0$ corresponds to the widely discussed scenario in which the quantum numbers are a copy of the ones of the SM leptons [16, 17, 20, 22, 23, 32, 48, 49]. In addition to a strong vacuum stability constraint, the $n = 0$ setup allows for direct mass mixing operators with the SM leptons. This can lead to large corrections of the couplings of the SM leptons with the weak gauge bosons and the Higgs and also induce tree level FCNC couplings. In addition, large 1-loop contributions to EDMs and MDMs can be generated. The measurements of EDMs, MDMs, lepton flavor violating observables and Z pole observables therefore constrain the coefficients of these mass mixing operators to be extremely small. One way to account for these bounds is to invoke a discrete symmetry which forbids mixing operators [16]. In the models considered in this article however, these operators are either absent in the $n = 2$ case, due to the different hypercharges between the vector-like and the SM leptons, or only one operator is allowed that couples the new sector just with the right handed SM sector, limiting the impact of the mass mixing operators for $n = 1$. In particular for $n = 1$, we find the following mass terms and Yukawa couplings,

$$\begin{aligned}
 -\Delta\mathcal{L} &= M_L \bar{L}_L \tilde{L}_R + M_E \tilde{\tilde{E}}_L E_R + y_E \tilde{L}_R h \tilde{E}_L + y_L \bar{L}_L h E_R \\
 &+ \sum_{\ell=e,\mu,\tau} y_\ell^{\text{SM}} \bar{\ell}_L h \ell_R + y_{L\ell} \bar{L}_L \tilde{h} \ell_R + h.c. ,
 \end{aligned} \tag{2}$$

in which SM fields are denoted by lower case letters, and $\tilde{h} \equiv i\sigma_2 h^\dagger$. Note that the hypercharge assignment only allows one mixing operator, that mixes the right-handed SM leptons with the left-handed doublet of vector leptons. The Lagrangian for the general scenario $n > 1$ corresponds to (2)

with the coefficient of the mixing operator set to zero, $y_{L\ell} = 0$. We only discuss the scenarios $n = 1$ and $n = 2$ here. Models with even higher hypercharges might lead to interesting phenomenology as well, but result in a Landau pole of the hypercharge gauge coupling at scales of $\sim 10^4$ TeV or below, see Section III B.

For $n = 2$, the new leptons carry electric charges $Q_E = -3$ and $Q_N = -2$. After electro-weak symmetry breaking (EWSB), the Lagrangian (2) leads to the following mass terms

$$-\Delta\mathcal{L} \supset (\bar{E}_L, \bar{\tilde{E}}_L) \mathbf{M}_E \begin{pmatrix} \tilde{E}_R \\ E_R \end{pmatrix} + \bar{N}_L \mathbf{M}_N \tilde{N}_R + m_\ell \bar{\ell}_L \ell_R + h.c. , \quad (3)$$

with the masses of the SM leptons $m_\ell = y_\ell^{\text{SM}} v$ and the Higgs vev, $v = 174$ GeV. In the absence of a doubly charged singlet, the mass of the charge two component of L will only be given by its vector mass, while the charge three leptons mix,

$$n = 2 : \quad \mathbf{M}_E = \begin{pmatrix} M_L & v y_L \\ v y_E^* & M_E \end{pmatrix} , \quad \mathbf{M}_N = M_L . \quad (4)$$

While the parameters M_L , M_E , y_L and y_E can all be complex, three phases can be absorbed by re-phasing the vector lepton fields, leaving one physical CP violating phase $\tilde{\phi} = \text{Arg}(M_L M_E y_L^* y_E)$. In the following we will work in a convention where the vector masses are real and positive and parametrize the physical phase by the relative phase of the Yukawa couplings, *i.e.* $\tilde{\phi} = \text{Arg}(y_L^* y_E)$.

For the case of $n = 1$, the new leptons carry electric charges $Q_E = -2$ and $Q_N = -1$, and the mass Lagrangian reads

$$-\Delta\mathcal{L} \supset (\bar{E}_L, \bar{\tilde{E}}_L) \mathbf{M}_E \begin{pmatrix} \tilde{E}_R \\ E_R \end{pmatrix} + (\bar{\ell}_L, \bar{N}_L) \mathbf{M}_N \begin{pmatrix} \ell_R \\ \tilde{N}_R \end{pmatrix} + h.c. , \quad (5)$$

Mixing with the SM leptons is generated proportional to the Yukawa couplings $y_{L\ell}$, so that

$$n = 1 : \quad \mathbf{M}_E = \begin{pmatrix} M_L & v y_L \\ v y_E^* & M_E \end{pmatrix} , \quad \mathbf{M}_N = \begin{pmatrix} v y_\ell^{\text{SM}} & 0 \\ v y_{L\ell} & M_L \end{pmatrix} , \quad (6)$$

in which only mixing with one SM lepton generation is considered for simplicity. The extension to the 3 generation case is straightforward. The phases of the mixing Yukawas $y_{L\ell}$ are additional physical sources of CP violation.

Both in the $n = 1$ and $n = 2$ case, we can diagonalize the mass matrix \mathbf{M}_E by a bi-unitary transformation $Z_L \mathbf{M}_E Z_R^\dagger = \text{diag}(m_1, m_2)$ and we introduce two Dirac spinors $(\chi_1, \chi_2)^T =$

$Z_L(E_L, \tilde{E}_L)^T + Z_R(\tilde{E}_R, E_R)^T$ to describe the light and heavy mass eigenstates with masses

$$m_{1,2}^2 = \frac{1}{2} \left(M_L^2 + M_E^2 + v^2(|y_E|^2 + |y_L|^2) \right. \\ \left. \mp \sqrt{(M_L^2 + M_E^2 + v^2(|y_E|^2 + |y_L|^2))^2 - 4|M_L M_E - v^2 y_L y_E^*|^2} \right). \quad (7)$$

In the $n = 2$ scenario, the charge two lepton $N = N_L + \tilde{N}_R$ is its own mass eigenstate with $m_N = M_L$. In the $n = 1$ scenario however, this is only true up to corrections proportional to the mixing coefficients $y_{L\ell}$. As we will see in the following, the size of the mixing between the SM leptons and the vector leptons is constrained to be small. We therefore treat this mixing perturbatively and find the following leading corrections to the masses of N and the SM leptons

$$m_N = M_L \left(1 + \frac{1}{2} \sum_{\ell} |y_{L\ell}|^2 \frac{v^2}{M_L^2} + \dots \right), \quad m_{\ell} = v y_{\ell}^{\text{SM}} \left(1 - \frac{1}{2} |y_{L\ell}|^2 \frac{v^2}{M_L^2} + \dots \right). \quad (8)$$

In the $n = 1$ case, the mixing terms also lead to modifications of the couplings of the SM leptons, once one rotates into the mass eigenstate basis. In particular, the flavor diagonal couplings of the Higgs to SM leptons and of the Z boson to right-handed SM leptons are modified at the order $|y_{L\ell}|^2 v^2 / M_L^2$. Moreover, flavor changing couplings of the Higgs to SM leptons and of the Z boson to right-handed SM leptons are induced at the same order, provided that the new leptons couple to at least two families of SM leptons simultaneously, see e.g. eqs. (B7) and (B11) in Appendix B. In addition, couplings of the W boson to the new charge one leptons and SM neutrinos as well as to the new charge 2 leptons and SM leptons are generated. Explicit expressions for all the couplings that are relevant for our analysis are collected in the Appendix B.

III. $H \rightarrow \gamma\gamma$, $H \rightarrow Z\gamma$, AND VACUUM INSTABILITY CONSTRAINTS

A. The $h \rightarrow \gamma\gamma$ Rate

Based on the mass matrices given in eqns. (4) and (6), one can obtain the contribution to the $h \rightarrow \gamma\gamma$ decay rate at leading order in the electro-weak scale over the vector masses, using low energy theorems [49–51]. Notice, that in contrast to the $n = 0$ scenario, for $n = 1$ there is only one off-diagonal mixing term between the vector-like and the SM leptons. As a consequence, both in the $n = 2$ and $n = 1$ scenarios, at leading order, the only non-SM contributions to the $h \rightarrow \gamma\gamma$ decay rate are generated by the mass matrix \mathcal{M}_E . In contrast to the case of chiral fermions, the effective interaction of the Higgs with photons contains both a CP-even and a CP-odd part [49]

$$\mathcal{L} \supset \frac{\alpha_{\text{em}}}{4\pi} Q_{\chi}^2 \frac{h}{v} \left(\frac{1}{3} F_{\mu\nu} F^{\mu\nu} \frac{\partial}{\partial \log v} \log \det \left(\mathcal{M}_E^{\dagger} \mathcal{M}_E \right) + \frac{1}{2} \epsilon^{\mu\nu\rho\sigma} F_{\mu\nu} F_{\rho\sigma} \frac{\partial}{\partial \log v} \arg \det \mathcal{M}_E \right). \quad (9)$$

As corrections to the Higgs production cross section are negligible in our framework, the ratio of the Higgs diphoton rate normalized to the respective SM rate is to an excellent approximation given by the ratio of the $h \rightarrow \gamma\gamma$ partial decay widths. We find

$$R_{\gamma\gamma} = \frac{\sigma(pp \rightarrow h)}{\sigma_{\text{SM}}(pp \rightarrow h)} \frac{\Gamma(h \rightarrow \gamma\gamma)}{\Gamma_{\text{SM}}(h \rightarrow \gamma\gamma)} \approx \frac{\Gamma(h \rightarrow \gamma\gamma)}{\Gamma_{\text{SM}}(h \rightarrow \gamma\gamma)} \approx \left| 1 + Q_\chi^2 \frac{4}{3} \frac{v \partial_v \log(\det \mathbf{M}_E^\dagger \mathbf{M}_E)}{A_1(\tau_W) + \frac{4}{3} A_{1/2}(\tau_t)} \right|^2 + \left| 4Q_\chi^2 \frac{v \partial_v \arg(\det \mathbf{M}_E)}{A_1(\tau_W) + \frac{4}{3} A_{1/2}(\tau_t)} \right|^2, \quad (10)$$

which is valid for both scenarios. Here, $\tau_i = 4m_i^2/m_h^2$ and we neglected the tiny bottom quark contribution to the SM width. To a good approximation, one has for the SM W and top loops $A_1(\tau_W) + \frac{4}{3} A_{1/2}(\tau_t) \approx -8.3 + 1.8 \approx -6.5$. Expressions for the loop functions A_1 and $A_{1/2}$ are collected in Appendix A. The explicit form of the derivatives of the mass matrix read

$$v \partial_v \log(\det \mathbf{M}_E^\dagger \mathbf{M}_E) = -4 \frac{M_E M_L \text{Re}(y_L^* y_E) v^2 - |y_E y_L|^2 v^4}{|M_E M_L - y_E^* y_L v^2|^2} \simeq -4 \frac{|y_L| |y_E| v^2}{M_E M_L} \cos \tilde{\phi}, \quad (11)$$

$$v \partial_v \arg(\det \mathbf{M}_E) = -2 \frac{M_L M_E \text{Im}(y_L^* y_E) v^2}{|M_E M_L - y_E^* y_L v^2|^2} \simeq -2 \frac{|y_L| |y_E| v^2}{M_E M_L} \sin \tilde{\phi}. \quad (12)$$

Note that the CP-odd contribution does not interfere with the SM amplitude. Even though the CP-odd part will therefore always enhance the $h \rightarrow \gamma\gamma$ cross section, it will typically amount to at most a percent correction for all phenomenologically viable parameters of the considered model. In Section IV, we will see that even this is very optimistic, given the very stringent bounds on the new physics phase, $\tilde{\phi}$, coming from the electron EDM. The CP-even part in (10) interferes with the SM contribution and therefore allows for significantly larger corrections. Depending on the overall sign of the numerator in (11), this can lead to an enhancement or decrease of the $h \rightarrow \gamma\gamma$ cross section. The term $\sim |y_E y_L|^2$ in (11) always leads to a decreased cross section compared to the SM, but can be neglected to a first approximation. The term could only become relevant for very small vector masses M_L and M_E , that are strongly constrained by direct searches, or for large Yukawa couplings, that are theoretically unattractive, as they imply large corrections to the running of the Higgs quartic coupling, forcing it to become negative at very low scales. The sign of the interference is therefore mainly determined by the sign of $\text{Re}(y_L^* y_E) = |y_L| |y_E| \cos \tilde{\phi}$.

While the expression (10) captures the leading contributions in an expansion in the ratio of the electro-weak scale over the vector masses, one can easily go beyond this approximation working with mass eigenstates of the new leptons. Doing so, the corrections to the Higgs diphoton decay rate can be written as

$$R_{\gamma\gamma} = \left| 1 + Q_\chi^2 \frac{\sum_i \frac{v}{m_i} \text{Re}(g_{h\chi_i\chi_i}) A_{1/2}(\tau_{\chi_i})}{A_1(\tau_W) + \frac{4}{3} A_{1/2}(\tau_t)} \right|^2 + \left| Q_\chi^2 \frac{\sum_i \frac{v}{m_i} \text{Im}(g_{h\chi_i\chi_i}) \tilde{A}_{1/2}(\tau_{\chi_i})}{A_1(\tau_W) + \frac{4}{3} A_{1/2}(\tau_t)} \right|^2. \quad (13)$$

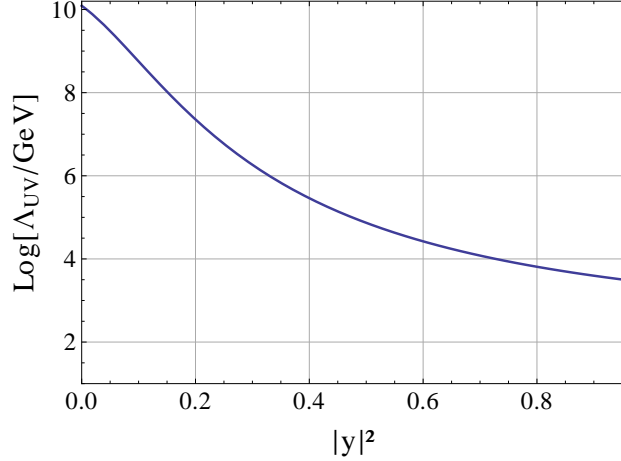


Figure 2. Scale at which the scalar quartic coupling turns negative due to renormalization group running, as function of the Yukawa couplings $|y| = |y_E| = |y_L|$.

The expressions for the couplings $g_{h\chi_i\chi_i}$ of the Higgs with the new lepton mass eigenstates are given in Appendix B. In the $n = 1$ case, there are in principle also contributions from the charge 1 leptons that are formally of higher order in v^2/M_L^2 . Working with mass eigenstates, they can be taken into account in a straight forward way. However, given the constraints on the mixing Yukawas that will be discussed in Section V, we find that contributions from the new charge 1 states are negligible even for very light masses $M_L = O(v)$. Expanding (13) in v/M we recover the approximate expression in (10). We find that (10) is accurate at the one percent level as long as the vector masses are $M_L, M_E \gtrsim 300$ GeV. In our numerical analysis, we work with mass eigenstates, though.

Due to their large charges, the new leptons can lead to sizable effects in $h \rightarrow \gamma\gamma$ even for moderate values of the Yukawa couplings. In particular, for fixed vector masses M_L and M_E , the Yukawa couplings can be smaller by a factor

$$y \rightarrow \frac{y}{Q_\chi}, \quad (14)$$

while keeping the decay rate constant compared to the $Q_\chi = 1$ ($n = 0$) scenario. Conversely, for fixed Yukawa couplings, higher charges allow for heavier vector masses.

B. Vacuum Stability

The existence of Yukawa type interactions, with order one couplings, of the Higgs with the new leptons has important implications for the stability of the Higgs potential. The Yukawa couplings

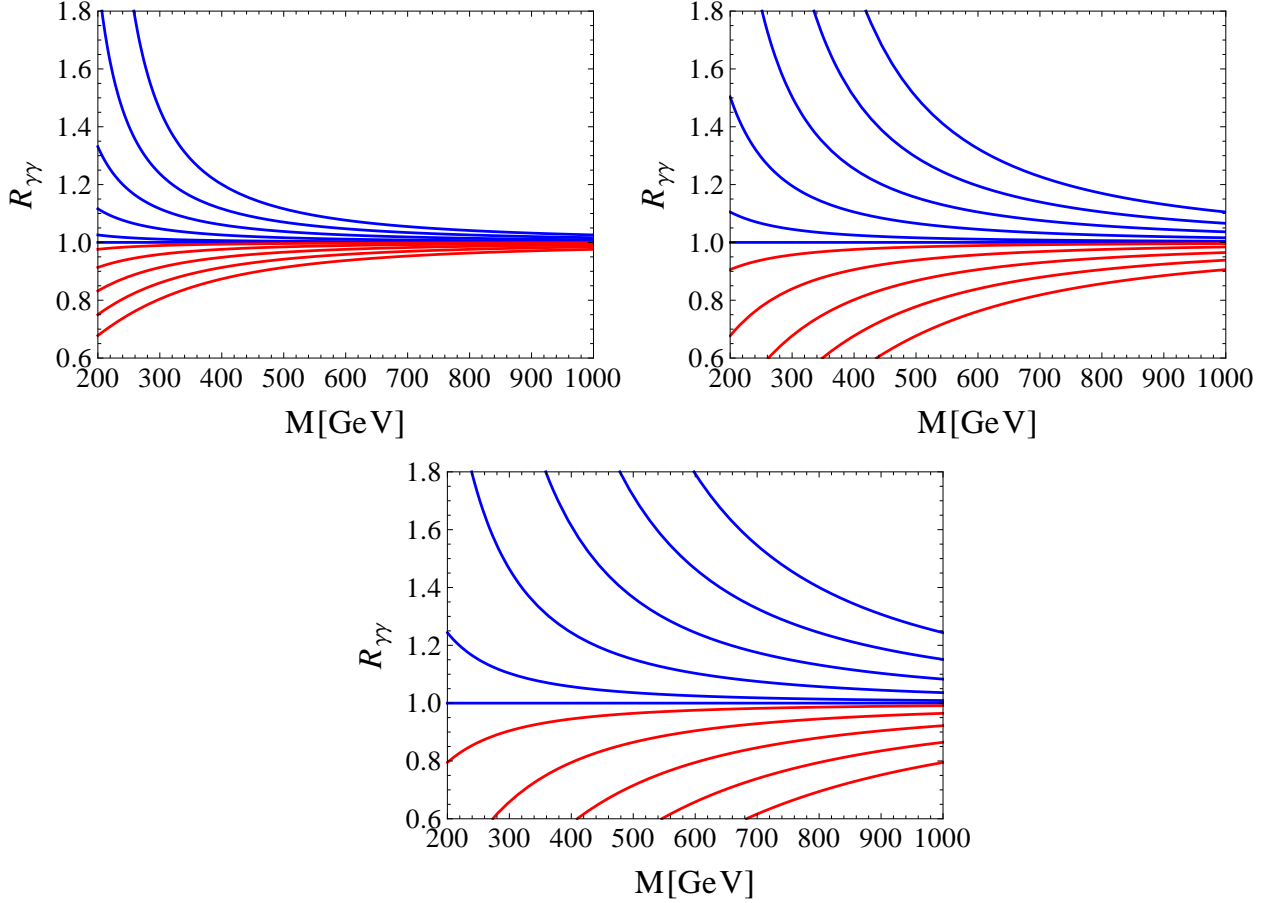


Figure 3. Modifications of the diphoton decay rate of the Higgs versus the vector mass $M = \sqrt{|M_E M_L|}$ for $n = 0$ and $n = 1$ on the upper left and right panel, as well as for $n = 2$ in the lower panel. The blue curves are for $\sqrt{y_E y_L} = \{0, 0.2, 0.4, 0.6, 0.8, 1\}$, and the red curves correspond to $\sqrt{-y_E y_L} = \{0.2, 0.4, 0.6, 0.8, 1\}$. For all three plots, $y_E = y_L = 0$ corresponds to $R_{\gamma\gamma} = 1$ and the effects become larger for larger absolute values of y_E and y_L .

contribute at 1-loop to the running of the Higgs quartic coupling through the box diagram on the right hand side of Figure 1. We find a correction to the SM beta function of¹

$$\frac{d\lambda}{dt} = \frac{1}{16\pi^2}\beta_\lambda = \frac{1}{16\pi^2}\left(\beta_\lambda^{\text{SM}} + 4\lambda(y_E^2 + y_L^2) - 4(y_E^4 + y_L^4)\right). \quad (15)$$

The scale at which the quartic coupling runs negative is plotted in Figure 2 versus the absolute value of the new Yukawa couplings $|y| = |y_E| = |y_L|$. For $y = 0$ one recovers the SM limit that, for values of $\alpha_s = 0.1184$ [52] and $m_t = 173.2$ GeV [53], and considering a two loop renormalization group running, yield a vanishing value of λ at a UV scale of $\Lambda_{\text{UV}} \simeq 10^{10}$ GeV (see e.g. [54, 55]).

¹ In the $n=1$ case there are additional contributions to the beta function coming from the mixing Yukawas $y_{L\ell}$. In regions of parameter space where the vector leptons can lead to sizable modifications of the $h \rightarrow \gamma\gamma$ rate, they are bound to be small from indirect constraints (see Section V). Therefore their impact on the running of the Higgs quartic is negligible.

The effect of non-zero Yukawa couplings $|y| = |y_E| = |y_L|$ on the vacuum stability of the Higgs potential has to be compared with the effects in $R_{\gamma\gamma}$, which are shown in Figure 3 as a function of the geometric mean of the vector masses $M = \sqrt{M_E M_L}$ for $n = 1$ in the upper right panel and for $n = 2$ in the lower panel. The $n = 0$ scenario is shown in the upper left panel for comparison. Each blue curve corresponds, from bottom to top, to Yukawa couplings $\sqrt{y_E y_L} = \{0, 0.2, 0.4, 0.6, 0.8, 1\}$, and each red curve corresponds, from top to bottom, to $\sqrt{-y_E y_L} = \{0.2, 0.4, 0.6, 0.8, 1\}$. For $y = 0$ one has $R_{\gamma\gamma} = 1$ and the effects are larger for larger absolute values of y . A possible phase $\tilde{\phi} = \text{Arg}(y_L^* y_E)$ is set to zero in the plots.

If one requires an enhancement of the Higgs diphoton rate by 30%, one finds in the $n = 0$ case that the Higgs quartic coupling runs negative at $\Lambda_{\text{UV}} \approx 10 - 100$ TeV, even for the most optimistic assumptions like the lightest mass eigenstate close to the LEP bound $m \sim 100$ GeV, in agreement with Ref. [17]. As a consequence, such models would require a UV completion at or below the 10-100 TeV scale. This bound can in principle be relaxed considerably for the scenarios considered in this work. For the same spectrum and the same enhancement of the Higgs diphoton rate, the scales where the Higgs quartic runs negative can be as high as 10^5 TeV in the $n = 1$ case and 10^6 TeV in the $n = 2$ case.² However, present LHC searches in multilepton channels, including taus, can already start probing the existence of new vector leptons. In the analyses presented in Section VI, we show that in the minimal models considered here, new vector leptons are viable if their vector masses are of the order of $M \gtrsim 370$ GeV in the case $n = 1$ and $M \gtrsim 850$ GeV in the case $n = 2$. Therefore, given that the vector leptons have to be considerably heavy in the minimal setups we have investigated, it turns out that the UV scale where the quartic Higgs coupling becomes negative is actually comparable to the $n = 0$ case, namely around $\sim 10 - 100$ TeV in the $n = 1$ case and even lower in the $n = 2$ case. As will be discussed in Section VI, in extensions of the setups with an additional massive neutral state and with additional interactions parametrized by higher dimensional operators, lighter vector-like leptons can become viable also for $n = 1$ and $n = 2$.

For the numerical calculation of the running we take into account the Higgs quartic, the SM gauge couplings, the top Yukawa and the contributions from the new Yukawas y_E and y_L . We use 2-loop expressions for the SM beta functions [56–60] and add the 1-loop contributions from the new leptons. The running of the Higgs quartic coupling was already given in (15). For the gauge and

² A comparable suppression of the Higgs di-photon rate requires slightly larger Yukawa couplings and therefore slightly smaller UV scales.

Yukawa couplings we find

$$\frac{dg_1}{dt} = \frac{g_1}{16\pi^2}\beta_1 = \frac{g_1}{16\pi^2} \left(\beta_1^{\text{SM}} + \frac{8}{3} \left(\frac{1}{2} + n \right)^2 g_1^2 + \frac{4}{3} (1+n)^2 g_1^2 \right), \quad (16)$$

$$\frac{dg_2}{dt} = \frac{g_2}{16\pi^2}\beta_2 = \frac{g_2}{16\pi^2} \left(\beta_2^{\text{SM}} + \frac{2}{3} g_2^2 \right), \quad (17)$$

$$\frac{dy_t}{dt} = \frac{y_t}{16\pi^2}\beta_t = \frac{y_t}{16\pi^2} \left(\beta_t^{\text{SM}} + |y_L|^2 + |y_E|^2 \right), \quad (18)$$

$$\frac{dy_L}{dt} = \frac{y_L}{16\pi^2}\beta_L = \frac{y_L}{16\pi^2} \left(\frac{3}{2} |y_L|^2 + (3y_t^2 + |y_L|^2 + |y_E|^2) - \left(\left[2n^2 + 3n + \frac{5}{4} \right] \frac{9}{5} g_1^2 + \frac{9}{4} g_2^2 \right) \right), \quad (19)$$

$$\frac{dy_E}{dt} = \frac{y_E}{16\pi^2}\beta_E = \frac{y_E}{16\pi^2} \left(\frac{3}{2} |y_E|^2 + (3y_t^2 + |y_L|^2 + |y_E|^2) - \left(\left[2n^2 + 3n + \frac{5}{4} \right] \frac{9}{5} g_1^2 + \frac{9}{4} g_2^2 \right) \right). \quad (20)$$

The beta function of the strong gauge coupling is not affected by the new uncolored states and we use $SU(5)$ normalization for the weak couplings $g_1^2 = \frac{5}{3}g^2$ and $g_2^2 = g'^2$. To first order in the ratio of the electro-weak scale over the vector masses, there is a direct correlation of contributions to the QED beta function and the CP-even coupling of the Higgs to two photons [14, 50, 51]. Therefore, a modification of $R_{\gamma\gamma}$ is necessarily correlated with a positive contribution to the running of the $SU(2)_L \times U(1)_Y$ gauge couplings. In particular, both in the $n = 1$ and $n = 2$ case, the running of the hypercharge leads to a Landau pole below the Planck scale, but for both scenarios, this Landau pole is orders of magnitude above the UV scale extracted from vacuum stability considerations in regions of parameter space with a sizable modification of $R_{\gamma\gamma}$. It should be mentioned, that this is not necessarily the case for scenarios with new leptons that carry even larger hypercharges. For example in the $n = 3$ case, the Landau pole arises already at a scale of $\sim 10^4$ TeV.

C. The $h \rightarrow Z\gamma$ Rate

The new vector-like leptons do not only contribute at the 1-loop level to the $h \rightarrow \gamma\gamma$ decay, but they also modify the $h \rightarrow Z\gamma$ rate. In the scenario where the new leptons have the same hypercharges as the SM leptons, their effect in $h \rightarrow Z\gamma$ is accidentally suppressed by $1 - 4s_W^2 \simeq 0.08$ and $h \rightarrow Z\gamma$ is to an excellent approximation SM-like [14]. This strong suppression does not arise for our non-standard hypercharge assignments, and larger effects can in principle be expected.

The corrections to the $h \rightarrow Z\gamma$ rate can be written in the following generic form

$$R_{Z\gamma} \simeq \frac{\Gamma(h \rightarrow Z\gamma)}{\Gamma_{\text{SM}}(h \rightarrow Z\gamma)} = \left| 1 + \frac{F_{\text{NP}}}{F_{\text{SM}}} \right|^2 + \left| \frac{\tilde{F}_{\text{NP}}}{F_{\text{SM}}} \right|^2. \quad (21)$$

Here, F_{SM} is the SM amplitude and F_{NP} (\tilde{F}_{NP}) is the CP conserving (CP violating) part of the NP amplitude. As in the case of $h \rightarrow \gamma\gamma$, the by far dominant NP contributions come from loops

involving the charge 2 states (for $n = 1$) or the charge 3 states (for $n = 2$), respectively. Working with mass eigenstates, we find

$$F_{\text{SM}} = \frac{1}{s_W c_W} \left[M_W^2 F_W + \left(2 - \frac{16}{3} s_W^2 \right) m_t^2 F_t \right] , \quad (22)$$

$$F_{\text{NP}} = Q_\chi \sum_{j,k} \frac{v}{m_j} F(m_j, m_k) \left[\text{Re}(g_{h\chi_k\chi_j}^* g_{Z\chi_k\chi_j}^L) + \text{Re}(g_{h\chi_j\chi_k} g_{Z\chi_k\chi_j}^R) \right] , \quad (23)$$

$$\tilde{F}_{\text{NP}} = Q_\chi \sum_{j,k} \frac{v}{m_j} G(m_j, m_k) \left[\text{Im}(g_{h\chi_j\chi_k} g_{Z\chi_k\chi_j}^R) - \text{Im}(g_{h\chi_k\chi_j}^* g_{Z\chi_k\chi_j}^L) \right] . \quad (24)$$

In the SM amplitude, we neglected the tiny contribution from the bottom quark loop. The W and top contributions, F_W and F_t , can be found for example in [61]. Numerically, we find approximately $M_W^2 F_W \simeq 5.1$ and $m_t^2 F_t \simeq -0.36$. The loop functions in the NP amplitudes are given by

$$F(m_j, m_k) = m_j^2 f(m_j, m_k, m_k) , \quad G(m_j, m_k) = m_j^2 g(m_j, m_k, m_k) , \quad (25)$$

with f and g given in [61]. The relevant couplings of the Higgs and the Z boson to the new lepton mass eigenstates are collected in Appendix B. Note that (23) and (24) contain contributions from loops where both mass eigenstates enter simultaneously. These contributions are parametrically of the same order as the contributions from loops that contain only one mass eigenstate.

In order to obtain an analytical understanding of the NP contributions to $h \rightarrow Z\gamma$, we expand the corrections to $R_{Z\gamma}$ to leading order in the electro-weak scale over the vector masses. We find

$$F_{\text{NP}} = -\frac{Q_\chi}{s_W c_W} \left[\left(1 + 4Q_\chi s_W^2 + h_1(x) \right) \frac{2}{3} \frac{|y_L||y_E|v^2}{M_L M_E} \cos \tilde{\phi} + h_2(x) \frac{(|y_L|^2 + |y_E|^2)v^2}{M_L^2} \right] , \quad (26)$$

$$\tilde{F}_{\text{NP}} = -\frac{Q_\chi}{s_W c_W} \left(1 + 4Q_\chi s_W^2 + h_3(x) \right) \frac{1}{3} \frac{|y_L||y_E|v^2}{M_L M_E} \sin \tilde{\phi} . \quad (27)$$

The functions h_1 , h_2 , and h_3 depend on the ratio of the vector masses $x = M_E^2/M_L^2$ and for degenerate masses we have $h_1(1) = h_2(1) = h_3(1) = 0$. The explicit expressions for the h_i functions are given in the appendix. Even for large splittings of the vector masses, we find that the effects of the h_i is typically small. Therefore, we indeed observe that in the $n = 0$ case, the corrections to $h \rightarrow Z\gamma$ are accidentally suppressed by $1 - 4s_W^2$, while such a suppression is absent in the $n = 1$ and $n = 2$ cases.

Figure 4 shows the correlation of NP effects in $h \rightarrow \gamma\gamma$ and $h \rightarrow Z\gamma$ for the 3 scenarios $n = 0, 1, 2$. In all the cases, the Yukawa couplings y_L and y_E are taken to be real and are varied between -1 and 1 . The vector masses M_L and M_E are allowed to vary in the ranges $200 - 400$ GeV, $400 - 600$ GeV, and $600 - 1000$ GeV for $n = 0$, $n = 1$, and $n = 2$, respectively. As expected, the modifications of the $h \rightarrow Z\gamma$ rate in the $n = 0$ scenario are on average small, and can reach at

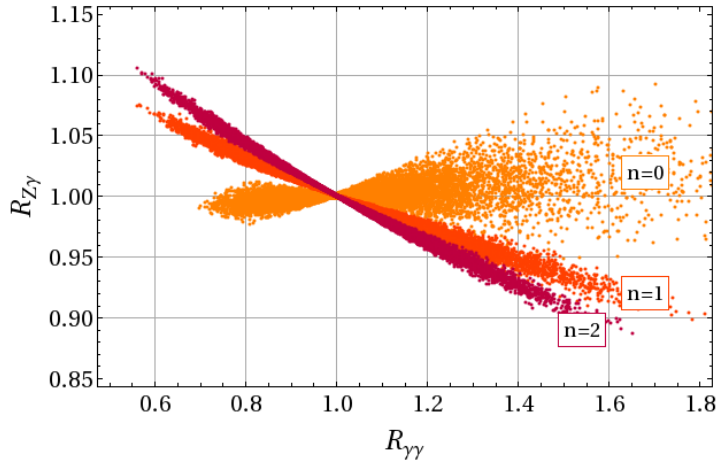


Figure 4. Correlations between the NP effects in $h \rightarrow \gamma\gamma$ and $h \rightarrow Z\gamma$ in the cases $n = 0$ (yellow), $n = 1$ (orange), and $n = 2$ (purple) as indicated.

most values between -5% to $+10\%$ for a strongly enhanced $h \rightarrow \gamma\gamma$ rate. For the scenarios with the larger hypercharges, the effects in $h \rightarrow Z\gamma$ can be slightly larger, but still typically do not exceed $\pm 10\%$, due to the fact that we have considered in each case values of the vector masses M that we expect could be compatible with direct LHC constraints on the vector-like fermions. The correlation of $R_{Z\gamma}$ and $R_{\gamma\gamma}$ is markedly distinct in the 3 cases, but NP effects in $h \rightarrow Z\gamma$ at the 10% level will be very challenging to probe at the LHC.

IV. CONSTRAINTS FROM ELECTRIC AND MAGNETIC DIPOLE MOMENTS AND ELECTRO-WEAK PRECISION OBSERVABLES

In addition to the need for a low UV cut-off, models in which the vector leptons share all quantum numbers with the SM leptons induce 1-loop contributions to SM fermion EDMs and MDMs. Measurements of these quantities result in very constraining limits, especially EDM measurements, which already probe electro-weak 2-loop contributions [62–65]. As a consequence, the mixing operators in these models must have very small coefficients or must be forbidden by an additional symmetry. Remarkably, in both scenarios discussed in this work, the leading contributions to EDMs and MDMs are automatically lifted to the 2-loop level.

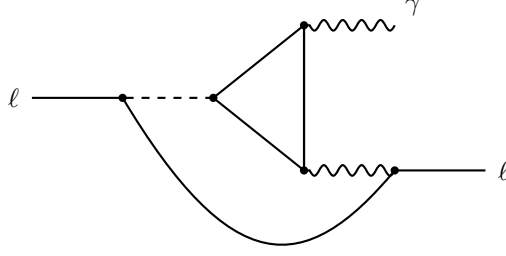


Figure 5. Barr Zee diagram with the Higgs diphoton sub-diagram, contributing to the EDM and MDM of SM leptons.

A. Electric Dipole Moments

For both $n = 1$ and $n = 2$, we can estimate contributions to the EDM of a SM fermion f by considering the 2-loop Barr-Zee type diagram in Figure 5, which contains the $h \rightarrow \gamma\gamma$ loop as a sub-diagram. Given that the Higgs couplings to the SM fermions are proportional to m_f/v , we obtain

$$\left(\frac{\Delta d_f}{e}\right)_{\text{Barr-Zee}} = \frac{\alpha_e Q_f Q_\chi^2}{8\pi^3} \frac{m_f}{v^2} \sum_i \frac{v}{m_i} \text{Im}(g_{h\chi_i\chi_i}) g\left(\frac{m_i^2}{m_h^2}\right). \quad (28)$$

The loop function g can be found in Appendix A. The source of this 2-loop EDM is the same as the CP violating contribution to $h \rightarrow \gamma\gamma$, namely the irreducible phase in the mass matrix \mathcal{M}_E . In the limit $m_i \gg v$ and for $M_L = M_E = M$ we can write

$$\left(\frac{\Delta d_f}{e}\right)_{\text{Barr-Zee}} \simeq \frac{\alpha_e Q_f Q_\chi^2}{8\pi^3} \frac{m_f}{v^2} [v \partial_v \arg(\det \mathcal{M}_E)] \frac{1}{2} \log\left(\frac{M^2}{m_h^2}\right), \quad (29)$$

thus making the correlation with the CP-odd contribution to the $h \rightarrow \gamma\gamma$ decay rate in (10) manifest. The explicit expression for the derivative was already given in (12). Note that the Barr-Zee contributions to the EDMs scale in the same way with the charge of the vector leptons, Q_χ , as the NP amplitude in $h \rightarrow \gamma\gamma$ does.

As we will show, bringing the 2-loop contributions in agreement with the most recent measurements of the electron EDM [62, 63],

$$d_e \leq 1.05 \times 10^{-27} \text{ e cm} \quad @ \text{ 90\% C.L.}, \quad (30)$$

still requires a fine-tuning of the phase of about 10%, in regions of parameter space that allow for a sizable modification of the CP conserving part of the $h \rightarrow \gamma\gamma$ amplitude, see e.g. Figure 7. Experimental results on EDMs of hadronic systems, e.g. the neutron EDM or mercury EDM [64, 65],

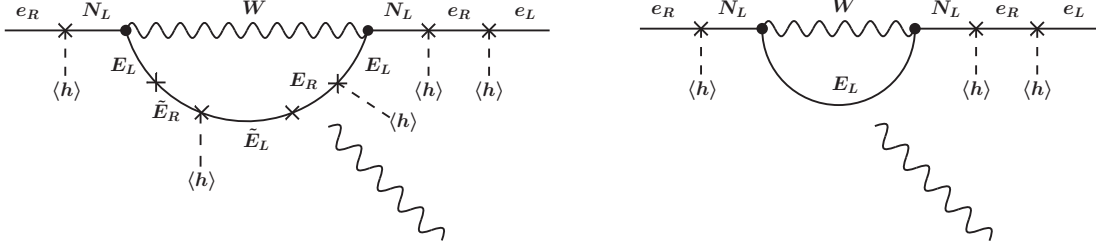


Figure 6. Example 1-loop diagrams giving rise to an electron EDM (left) and MDM (right) in the $n = 1$ scenario. The photon can be attached to all charged particles in the loops

lead to constraints on quark EDMs that translate into comparable bounds on the model parameters, but they are subject to large hadronic uncertainties. Note, that additional diagrams with the internal $h\gamma$ replaced by a hZ can be important for quark EDMs, but will play essentially no role for leptons because of the accidentally small vector coupling of the Z to SM leptons. 2-loop diagrams with W^+W^- in the loop turn out to be small for both quarks and leptons, see also [23]. Nonetheless, in our numerical analysis, we take into account the full set of $h\gamma$, hZ , and W^+W^- contributions.

The mixing operator in the $n = 1$ scenario also allows for an additional 1-loop contribution to the SM lepton EDMs. As the new states only mix with right-handed SM leptons, the physical phases in the mixing Yukawas cannot be accessed at the 1-loop level. The only possible 1-loop contribution is therefore a loop of a W boson and charge two vector leptons that is sensitive to the phase in the charge 2 mass matrix \mathcal{M}_E . This 1-loop EDM corresponds to a dimension 10 operator, containing 5 Higgs fields (see diagram on the left hand side of Figure 6). It can only compete with the 2-loop dimension 6 contribution if $|y_{L\ell}| = \mathcal{O}(1)$ and $M_L, M_E \simeq v$. Given the constraints on the mixing Yukawas discussed in Section V, we find that the 1-loop contribution is completely negligible.

Figure 7 illustrates the impact of the electron EDM bound on a modified $h \rightarrow \gamma\gamma$ rate. Shown are modifications of the Higgs diphoton rate in the $|y_L| = |y_E|$ vs $\tilde{\phi} = \text{Arg}(y_L^* y_E)$ plane. The left (right) plot shows the $n = 1$ ($n = 2$) case with the mass of the vector leptons fixed to exemplary values of $M = M_L = M_E = 500$ GeV (900 GeV). The parameter space ruled out by EDMs generated from the 2-loop Barr-Zee diagrams is shown in orange. Away from the limits $M_L = M_E$ and $|y_L| = |y_E|$, the results do not change qualitatively. We observe that $\mathcal{O}(1)$ phases are allowed, but only for small values of the couplings that cannot lead to any appreciable modification of the $h \rightarrow \gamma\gamma$ rate. A non-negligible modification of $h \rightarrow \gamma\gamma$ is only possible if the phase is at most at the level of 0.1. Correspondingly, a CP-odd contribution to the $h \rightarrow \gamma\gamma$ rate at the percent level would already be in

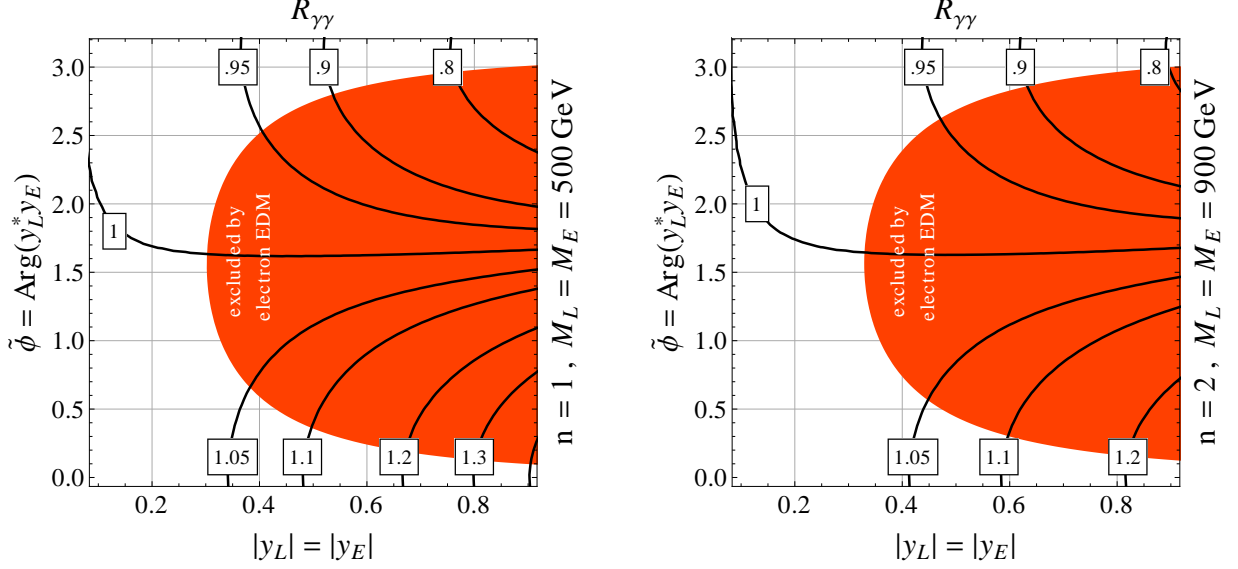


Figure 7. Modifications of the $h \rightarrow \gamma\gamma$ rate in the $|y| - \tilde{\phi}$ plane in the $n = 1$ (left) and $n = 2$ (right) scenarios. Vector masses are fixed to 500 GeV and 900 GeV, respectively. The region excluded by the electron EDM is shown in orange.

conflict with EDMs, barring accidental cancellations with contributions induced by additional CP violating sources from beyond the models considered here. This agrees with the findings in [23, 32]. Analogously, EDM bounds also strongly restrict possible CP violating effects in $h \rightarrow Z\gamma$ well below the percent level. Possible CP violation in the experimentally most favorable $h \rightarrow ZZ$ channel is even further suppressed below the 10^{-4} level, because loop induced CP violating effects have to compete with the CP conserving tree level hZZ coupling. Since the imaginary part of the couplings is constrained to be very small, we will only work with real y_L and y_E couplings for the remainder of this paper.

B. Anomalous Magnetic Moments

The 2-loop Barr-Zee diagrams also give contributions to anomalous magnetic moments of leptons in both scenarios

$$(\Delta a_\ell)_{\text{Barr-Zee}} = \frac{\alpha_e Q_\chi^2}{4\pi^3} \frac{m_\ell^2}{v^2} \sum_i \frac{v}{m_i} \text{Re}(g_{h\chi_i\chi_i}) f\left(\frac{m_i^2}{m_h^2}\right). \quad (31)$$

with the explicit form of the 2-loop function f given in Appendix A. In the limit $m_i \gg v$ and for $M_L = M_E = M$ we can write

$$(\Delta a_\ell)_{\text{Barr-Zee}} \simeq \frac{\alpha_e Q_\chi^2}{4\pi^3} \frac{m_\ell^2}{v^2} [v \partial_v \log(\det \mathcal{M}_E^\dagger \mathcal{M}_E)] \frac{1}{3} \log\left(\frac{M^2}{m_h^2}\right). \quad (32)$$

This shows clearly the correlation of the anomalous magnetic moments with the CP-even contributions to the $h \rightarrow \gamma\gamma$ decay rate. The explicit expression for the derivative can be found in (11).

However, given the uncertainty of the current experimental results and the precision of the SM predictions [66]

$$\Delta a_\mu = a_\mu^{\text{exp}} - a_\mu^{\text{SM}} = (2.9 \pm 0.9) \times 10^{-9}, \quad (33)$$

$$\Delta a_e = a_e^{\text{exp}} - a_e^{\text{SM}} = (-10.5 \pm 8.1) \times 10^{-13}, \quad (34)$$

we find that the 2-loop contributions lead to effects that are one order of magnitude below the current sensitivities or even smaller, even for vector masses at the order of the electro-weak scale and Yukawa couplings of order 1.

In the $n = 1$ scenario, there are in addition various 1-loop contributions coming from Higgs, W and Z exchange between the SM and the vector leptons. In contrast to the 1-loop contribution to the EDMs, the 1-loop MDMs correspond to dimension 8 operators (see the example diagram on the right hand side in Figure 6). Nevertheless, we find that only for $M_L, M_E \sim v$ and $y_{L\ell} = \mathcal{O}(1)$ can 1-loop MDMs reach the current sensitivities. For all realistic choices of parameters, all contributions to the MDMs are negligible in our models.³

C. S and T Parameter

Additional constraints on the discussed scenarios arise from electro-weak precision observables, in particular the S and T parameters. The latest constraints on S and T read [68]

$$\Delta S = 0.03 \pm 0.10, \quad \Delta T = 0.05 \pm 0.12, \quad (35)$$

with a strong positive correlation between the two parameters of +0.89. In our setups, contributions to S and T arise at 1-loop and at order $\mathcal{O}(y^4 v^2/M^2)$, with $M \sim M_L, M_E$ and $y \sim y_L, y_E$.

Contributions to the T parameter are independent of the hypercharge of the new vector-like leptons. The T parameter leads only to weak constraints on the masses M_L and M_E and the

³ Sizable contributions to the anomalous magnetic moments of leptons can arise in models where the vector-like leptons have the same quantum numbers as the SM leptons [42, 67].

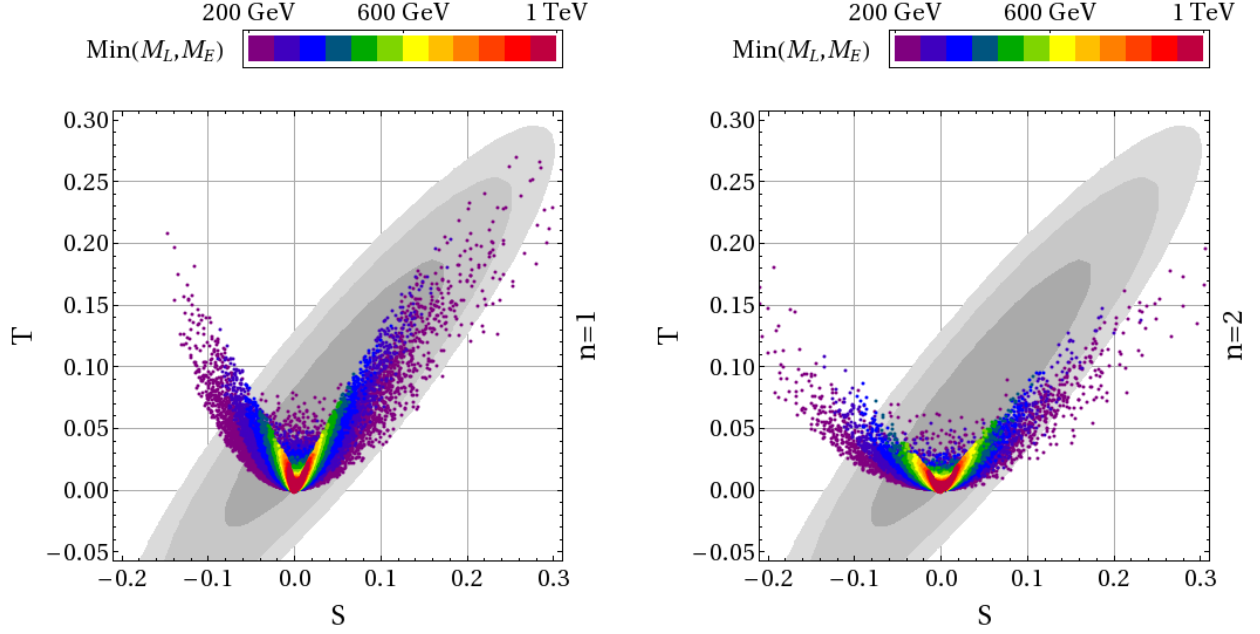


Figure 8. Contributions to the S and T parameters from the new vector-like leptons for $n = 1$ (left plot) and $n = 2$ (right plot). In both plots, the Yukawa couplings are varied in the range $-1 < y_E, y_L < 1$. The color code indicates the value of the lighter of the vector masses. The region allowed by the electro-weak precision fit is shown with the gray ellipses at the 1, 2, and 3σ level.

Yukawa couplings y_E and y_L . Even for sizable Yukawas, $y_E = y_L = 1$, vector masses as low as $M_L = M_E = 300$ GeV are allowed [20]. Contributions to the S parameter do depend on the hypercharge assignments. We calculate corrections to the S parameter in our scenarios by adapting the general expressions given in [69]. We find that despite the large hypercharges, corrections to the S parameter are typically also moderate.

This is illustrated in Figure 8 which shows the contributions to the S and T parameters from the new vector-like leptons for $n = 1$ (left plot) and $n = 2$ (right plot). In both plots, the Yukawa couplings are varied independently in the range $-1 < y_E, y_L < 1$ and the vector masses are $M_L, M_E > 200$ GeV. The color code indicates the value of the lighter of the vector masses. The region allowed by the electro-weak precision fit [68] is shown with the gray ellipses at the 1, 2, and 3σ level. In the regions of parameter space that are not excluded in the minimal models by direct searches ($M_L, M_E \gtrsim 370$ GeV for $n = 1$ and $M_L, M_E \gtrsim 850$ GeV for $n = 2$, see Section VI), we typically have very small corrections, $\Delta T \lesssim 0.05$ and $\Delta S \lesssim 0.05$, well within the range allowed by the precision electro-weak fit. We find that the S and T parameter can lead to non-trivial constraints only for very small vector masses of ~ 200 GeV–300 GeV.

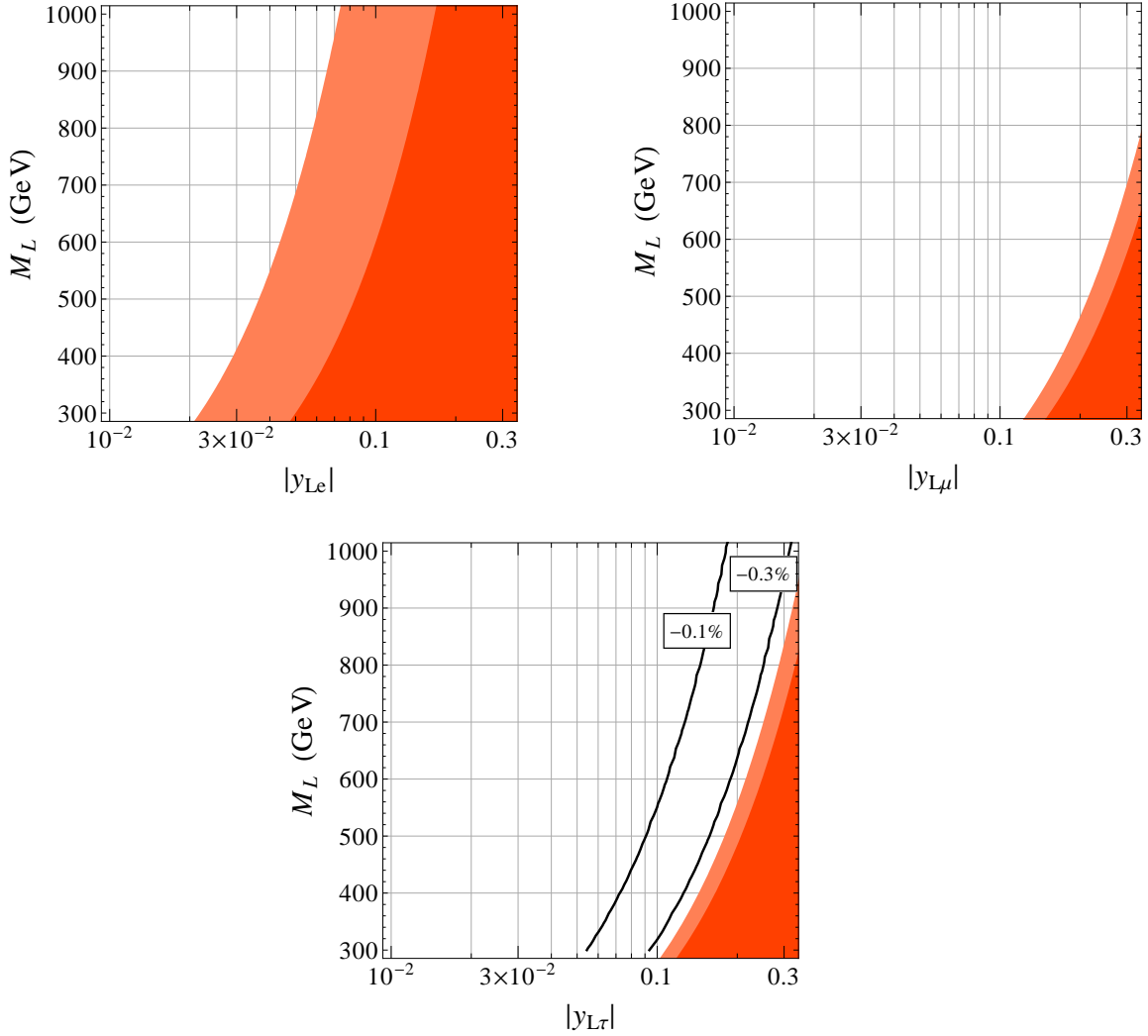


Figure 9. Constraints from the LEP measurements of the Z boson couplings in the plane of the vector lepton mass M_L and the mixing Yukawa couplings $y_{L\ell}$ with electrons (top left), muons (top right), and taus (bottom). The light (dark) orange regions are excluded at the 2σ (3σ) level. In the bottom plot, modifications of the $h \rightarrow \tau\tau$ rate are also shown with the black contours.

V. CONSTRAINTS ON MIXING WITH THE STANDARD MODEL LEPTONS

In the $n = 1$ case, the mixing between the SM leptons and the new leptons is subject to strong indirect constraints from Z pole observables and lepton flavor violating processes. In this section, we discuss the most stringent constraints and their implications.

A. Constraints from Modified Z and Higgs Couplings

The couplings of the SM leptons to the Z boson have been precisely measured at LEP. As already mentioned at the end of Section II, the Yukawa couplings that mix the SM leptons with the new particles lead to corrections to the coupling of the Z with the right-handed SM leptons. Such corrections are constrained at the 10^{-3} level and better [70]. Combining the experimental results with the SM predictions collected in [70] we find

$$\delta g_{Re} = |y_{Le}|^2 \frac{v^2}{2M_L^2} = -0.00060 \pm 0.00034 , \quad (36)$$

$$\delta g_{R\mu} = |y_{L\mu}|^2 \frac{v^2}{2M_L^2} = 0.0002 \pm 0.0013 , \quad (37)$$

$$\delta g_{R\tau} = |y_{L\tau}|^2 \frac{v^2}{2M_L^2} = 0.00066 \pm 0.00064 , \quad (38)$$

where the $\delta g_{R\ell}$ are defined as the relative deviations of the coupling of the Z with the right-handed SM leptons

$$\mathcal{L} \supset -\frac{e}{s_W c_W} Z^\mu \bar{\ell} \gamma_\mu \left[(g_{L\ell}^{\text{SM}} + \delta g_{L\ell}) P_L + (g_{R\ell}^{\text{SM}} + \delta g_{R\ell}) P_R \right] \ell . \quad (39)$$

The model predicts always positive corrections to the couplings $g_{R\ell}$. As the measured coupling of electrons is almost 2σ below the SM prediction, the derived constraints are particularly strong in the case of electrons. The constraints are illustrated in the plots of Figure 9 in the M_L - $y_{L\ell}$ planes. Dark and light orange regions are excluded at the 3σ and 2σ level, respectively.

There can in principle be also corrections to the decay of the Higgs to leptons. We find at leading order the following modification of the $h \rightarrow \tau\tau$ signal strength

$$R_{\tau\tau} \simeq \frac{\Gamma(h \rightarrow \tau\tau)}{\Gamma(h \rightarrow \tau\tau)_{\text{SM}}} \simeq 1 - |y_{L\tau}|^2 \frac{v^2}{M_L^2} . \quad (40)$$

Contours of constant $R_{\tau\tau}$ are superimposed in the bottom plot of Figure 9. Given the constraints from the Z pole measurements, this correction is unobservably small. This is in contrast to the $n = 0$ case where the additionally allowed mixing Yukawas and masses can lead to visible modifications of Higgs couplings to fermions [20].

B. Lepton Flavor Violation

Very stringent constraints on the coefficients of the mixing operators in the $n = 1$ Lagrangian also come from observables measuring the flavor changing couplings of the Z . The most severe bounds

result from the tree-level induced $\mu \rightarrow e$ conversion in nuclei, and flavor violating τ decays, like $\tau \rightarrow 3e$ and $\tau \rightarrow 3\mu$.

For the $\mu \rightarrow e$ conversion in nuclei, the branching ratio can be written as [71]

$$\text{BR}(\mu \rightarrow e \text{ in } N) \times \omega_{\text{cap.}}^N = 4 \left| (2C_u + C_d)V^{(p)} + (C_u + 2C_d)V^{(n)} \right|^2, \quad (41)$$

in which $\omega_{\text{cap.}}^N$ denotes the muon capture rate of the nucleus N , and $V^{(p)}$ and $V^{(n)}$ are nucleus dependent overlap integrals [71].

The coefficients C_u and C_d are defined by the effective Hamiltonian

$$\mathcal{H} = C_q (\bar{e} \gamma_\nu P_R \mu) (\bar{q} \gamma^\nu q), \quad (42)$$

and are generated by off-diagonal Z couplings. We find

$$C_u = y_{L\mu} y_{Le}^* \frac{1}{4M_L^2} \left(1 - \frac{8}{3} s_W^2 \right), \quad C_d = -y_{L\mu} y_{Le}^* \frac{1}{4M_L^2} \left(1 - \frac{4}{3} s_W^2 \right). \quad (43)$$

The current most stringent experimental bounds are coming from measurements using Au and Ti atoms [72, 73]

$$\text{BR}(\mu \rightarrow e \text{ in Au}) < 7 \times 10^{-13} \quad @ 90\% \text{ C.L.}, \quad (44)$$

$$\text{BR}(\mu \rightarrow e \text{ in Ti}) < 1.7 \times 10^{-12} \quad @ 90\% \text{ C.L.}, \quad (45)$$

and can be translated into bounds on the combinations of couplings, which enter (43).

The corresponding parameter space is shown in Figure 10, with the excluded region shaded in orange. Generically, for $y_{Le} \simeq y_{L\mu}$, couplings at the order of 10^{-3} are probed. However, as only the product of these two couplings is constrained, either of the couplings can be as large as the bound obtained from Z pole observables in the previous section, as long as the other coupling is strongly suppressed. The expected sensitivity of the Mu2e experiment to $\mu \rightarrow e$ conversion in Al, $\text{BR}(\mu \rightarrow e \text{ in Al}) \lesssim 6 \times 10^{-17}$ [74], will probe large regions of the presently allowed parameter space.

For $\ell \rightarrow 3\ell'$ decays, the branching ratio can be written as

$$\frac{\text{BR}(\ell \rightarrow 3\ell')}{\text{BR}(\ell \rightarrow \ell' \nu \bar{\nu})} = \frac{1}{4G_F^2} \left(|C_{LL}|^2 + |C_{RR}|^2 + \frac{1}{2}|C_{RL}|^2 + \frac{1}{2}|C_{LR}|^2 \right), \quad (46)$$

where the coefficients C_i are defined by the effective Hamiltonian

$$\begin{aligned} \mathcal{H} = & -C_{LL} (\bar{\ell}' \gamma_\nu P_L \ell) (\bar{\ell}' \gamma^\nu P_L \ell') - C_{RR} (\bar{\ell}' \gamma_\nu P_R \ell) (\bar{\ell}' \gamma^\nu P_R \ell') \\ & - C_{LR} (\bar{\ell}' \gamma_\nu P_L \ell) (\bar{\ell}' \gamma^\nu P_R \ell') - C_{RL} (\bar{\ell}' \gamma_\nu P_R \ell) (\bar{\ell}' \gamma^\nu P_L \ell'). \end{aligned} \quad (47)$$

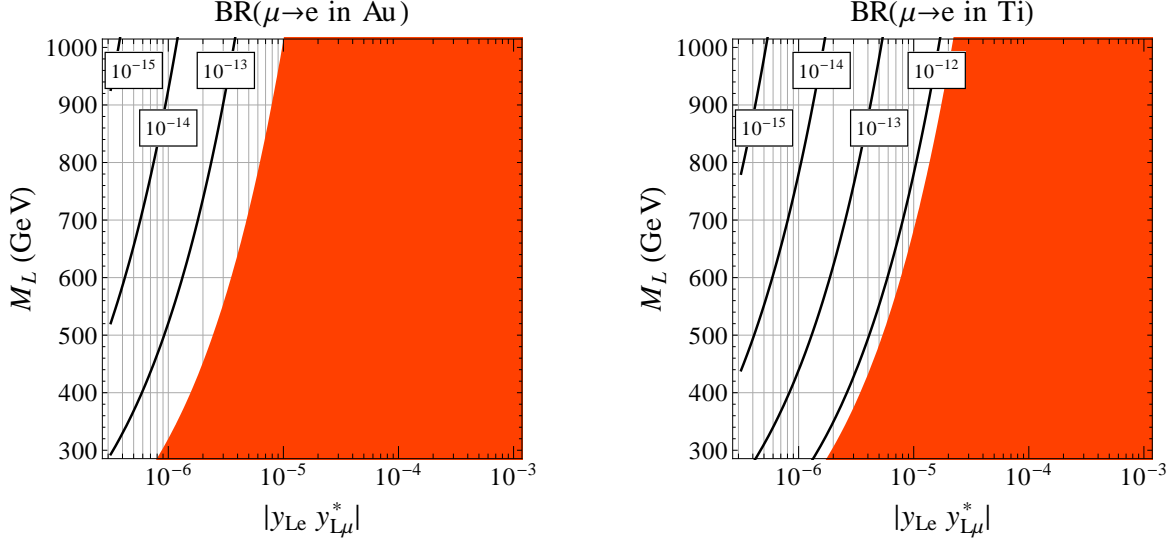


Figure 10. The branching ratios of $\mu \rightarrow e$ conversion in gold (left) and titanium (right) as function of the mass of the new vector-like fermions and the relevant combination of couplings. The orange regions are excluded by current constraints.

The dominant contribution comes again from the tree level exchange of the Z boson with its flavor violating coupling to right-handed leptons. We have

$$C_{RR} = y_{L\ell} y_{L\ell'}^* \frac{1}{M_L^2} s_W^2, \quad C_{RL} = y_{L\ell} y_{L\ell'}^* \frac{1}{2M_L^2} (2s_W^2 - 1), \quad (48)$$

and contributions to C_{LL} and C_{LR} are negligible, see eq. (B10). The resulting branching ratio for $\mu \rightarrow 3e$ gives a weaker bound than $\mu \rightarrow e$ conversion, while the $\tau \rightarrow 3e$ and $\tau \rightarrow 3\mu$ branching ratios allow to constrain the mixing of the vector-like leptons with the τ .

The current bounds on the τ branching ratios are [75]

$$\text{BR}(\tau \rightarrow 3e) < 2.7 \times 10^{-8} \quad @ 90\% \text{ C.L.}, \quad (49)$$

$$\text{BR}(\tau \rightarrow 3\mu) < 2.1 \times 10^{-8} \quad @ 90\% \text{ C.L.}. \quad (50)$$

The allowed parameter space is shown in Figure 11, again with the experimentally excluded region shaded in orange. Other flavor violating leptonic tau decays like $\tau^+ \rightarrow e^+ \mu^+ \mu^-$, $\tau^+ \rightarrow \mu^+ e^+ e^-$, or lepton flavor violating semi-leptonic tau decays lead to very similar constraints. Bounds from the loop induced $\ell \rightarrow \ell' \gamma$ decays constrain the same combination of couplings as the observables discussed previously, but – due to the loop suppression – result in much weaker constraints, so that we refrain from presenting a detailed discussion of these bounds.

Note that due to the strong constraint from $\mu \rightarrow e$ conversion either $\tau \rightarrow 3e$ or $\tau \rightarrow 3\mu$ can be close to the current bound, but not both simultaneously. Indeed, combining the expressions for

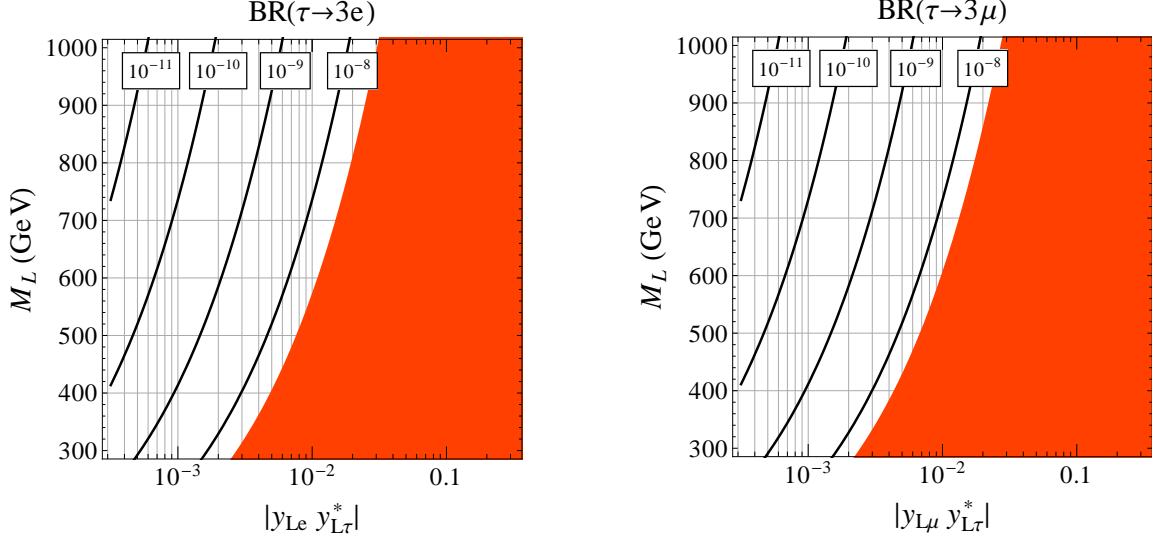


Figure 11. The branching ratios of $\tau \rightarrow 3e$ (left), and $\tau \rightarrow 3\mu$ (right) as function of the mass of the new vector-like fermions and the relevant combination of couplings. The orange regions are excluded by current constraints.

$\text{BR}(\tau \rightarrow 3e)$, $\text{BR}(\tau \rightarrow 3\mu)$, $\text{BR}(\mu \rightarrow e \text{ in Au})$, and $\delta g_{R\tau}$, we arrive at the following relation that is independent of any model parameters

$$\text{BR}(\tau \rightarrow 3e) \times \text{BR}(\tau \rightarrow 3\mu) = \text{const.} \times (\delta g_{R\tau})^2 \times \text{BR}(\mu \rightarrow e \text{ in Au}) . \quad (51)$$

The proportionality constant is purely given by known SM parameters, and we find: $\text{const.} \simeq 1.2 \times 10^{-4}$. The constraint from $\mu \rightarrow e$ conversion on possible NP effects in $\text{BR}(\tau \rightarrow 3e)$ and $\text{BR}(\tau \rightarrow 3\mu)$ is illustrated in Figure 12. Shown in orange is the region in the $\text{BR}(\tau \rightarrow 3e)$ vs. $\text{BR}(\tau \rightarrow 3\mu)$ plane that is excluded by the current bound on $\text{BR}(\mu \rightarrow e \text{ in Au})$, allowing a correction to $\delta g_{R\tau}$ that saturates the experimental 2σ upper limit. The diagonal lines indicate the values for $\mu \rightarrow e$ conversion in Al, in the still allowed regions. The expected sensitivity of the Mu2e experiment to $\text{BR}(\mu \rightarrow e \text{ in Al})$ is shown with the orange dashed line. The current experimental constraints on $\text{BR}(\tau \rightarrow 3e)$ and $\text{BR}(\tau \rightarrow 3\mu)$ are shown with the horizontal and vertical black dotted lines. Finding both $\text{BR}(\tau \rightarrow 3e)$ and $\text{BR}(\tau \rightarrow 3\mu)$ close to the current bounds would clearly rule out the studied framework.

In conclusion, observables measuring deviations of the Z couplings to SM leptons lead to constraints on the mixing Yukawas in the $n = 1$ case. The strongest bounds are summarized in Table I. The analysis in this section has to be contrasted with the results from studies of models of new vector-like leptons, which have the exact same quantum numbers as their SM cousins. In these models, highly non-generic CP and flavor structures are necessary in order to satisfy the constraints

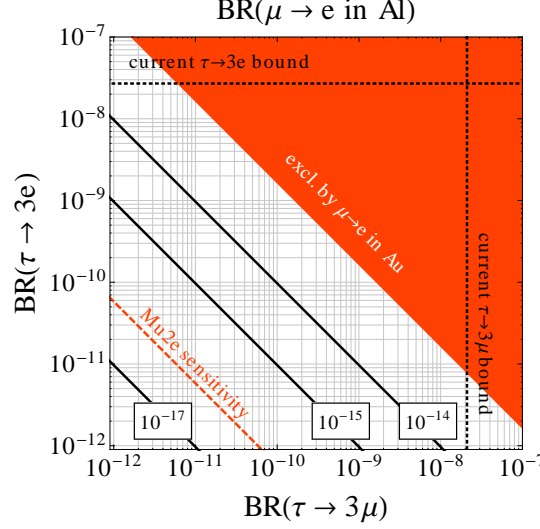


Figure 12. Contours of constant $\text{BR}(\mu \rightarrow e \text{ in Al})$ in the $\text{BR}(\tau \rightarrow 3e)$ vs $\text{BR}(\tau \rightarrow 3\mu)$ plane. The orange region is excluded by the current $\text{BR}(\mu \rightarrow e \text{ in Au})$ constraint. The current bounds on $\text{BR}(\tau \rightarrow 3e)$ and $\text{BR}(\tau \rightarrow 3\mu)$ are indicated with the black dotted lines. The sensitivity of the Mu2e experiment is shown with the orange dashed line.

$\text{BR}(\mu \rightarrow e \text{ in Au})$	$\left \frac{v^2}{M_L^2} y_{Le} y_{L\mu} < 0.3 \times 10^{-6} \right.$	δg_{Re}	$\left \frac{v^2}{M_L^2} y_{Le} ^2 < 1.6 \times 10^{-4} \right.$
$\text{BR}(\tau \rightarrow 3e)$	$\left \frac{v^2}{M_L^2} y_{Le} y_{L\tau} < 0.9 \times 10^{-3} \right.$	$\delta g_{R\mu}$	$\left \frac{v^2}{M_L^2} y_{L\mu} ^2 < 5.6 \times 10^{-3} \right.$
$\text{BR}(\tau \rightarrow 3\mu)$	$\left \frac{v^2}{M_L^2} y_{L\mu} y_{L\tau} < 0.8 \times 10^{-3} \right.$	$\delta g_{R\tau}$	$\left \frac{v^2}{M_L^2} y_{L\tau} ^2 < 3.9 \times 10^{-3} \right.$

Table I. Summary of the strongest bounds on the mixing Yukawas from lepton flavor violating processes (left) and Z pole observables (right).

discussed in this section, see for example [66] and references therein.

VI. COLLIDER PHENOMENOLOGY

A. Production of the Vector-Like Leptons

In both scenarios, the new vector leptons will dominantly be pair produced in Drell–Yan processes due to their large hypercharges. Sub-dominant channels are Higgs mediated pair production or the production of a pair of vector-like leptons with different charges through a W .

In the $n = 1$ scenario, the W channel does also allow for a charge 2 vector-like lepton to be produced together with a charged SM lepton, or for the charge 1 vector-like lepton to be produced

together with a SM neutrino. For $n = 1$, there is also Drell-Yan production of a charge 1 vector-like lepton together with a charged SM lepton. The single production channels are however suppressed by the Yukawa matrix $y_{L\ell}$, which parametrizes the mixing of the vector leptons with the SM leptons, as well as by powers of the electro-weak scale over the vector masses. They turn out to be two to three orders of magnitude smaller compared to the Drell-Yan production at the current LHC energy $\sqrt{s} = 8$ TeV.

B. Decays of the Vector-Like Leptons: $n = 2$ Case

In the minimal $n = 2$ scenario, the hypercharge assignments do not allow for a coupling between the new vector leptons and the SM leptons. Therefore, the lightest charge three state is stable, because it cannot decay into SM fields if one considers the theory to be renormalizable. Higher dimensional operators have to be considered within the model to allow for the decay of the lightest charge 3 state.

The lowest dimensional operators that can lead to a decay of the charge three states into SM particles are of dimension six, namely ⁴

$$\begin{aligned} \Delta\mathcal{L} \ni & \frac{(c_R)_{ijk}}{\Lambda^2} \bar{E}_R \ell_R^i \ell_R^j \ell_R^k + \frac{(c_L)_{ijk}}{\Lambda^2} \bar{E}_L \ell_R^i \ell_R^j \ell_L^k \\ & + \frac{(\tilde{c}_R)_{ijk}}{\Lambda^2} \bar{\tilde{E}}_R \ell_R^i \ell_R^j \ell_L^k + \frac{(\tilde{c}_L)_{ijk}}{\Lambda^2} \bar{\tilde{E}}_L \ell_R^i \ell_R^j \ell_R^k, \end{aligned} \quad (52)$$

in which a summation over lepton flavor $\ell^i, \ell^j, \ell^k = e, \mu, \tau$ is implicit. These operators violate SM lepton number and generically also lepton flavor. Dimension six operators that would allow proton decay must obviously be further suppressed, which can be achieved through a UV completion that does not couple leptons to colored fermions or conserves baryon number. The most stringent bounds from dimension six operators, which directly contribute to charged lepton flavor violating (LFV) processes, point to a new physics scale of $\Lambda > 10^3$ TeV [78]. If Λ is smaller, bounds from LFV processes call for additional flavor structure in the corresponding Wilson coefficients.

Considering no additional structure in the Wilson coefficients $(c_L)_{ijk} \approx (c_R)_{ijk} = \mathcal{O}(1)$, the lifetime and decay length of the vector leptons can be approximated by

$$\tau = \frac{1}{n} \frac{192\pi^3}{m_{\chi_\ell}^5} \Lambda^4 \approx 0.2 \text{ mm} \left(\frac{\Lambda}{10^3 \text{ TeV}} \right)^4 \left[\frac{800 \text{ GeV}}{m_{\chi_\ell}} \right]^5, \quad (53)$$

where a combinatorial factor $n = 27$, which counts the different SM lepton flavor variations that can appear in the operators (52), has been taken into account. If the scale of new physics Λ is

⁴ Note, that new leptons with even larger hypercharges can only decay through operators with dimension eight or higher.

sufficiently large, $\Lambda \gg 10^3$ TeV, the new states can behave as stable particles within the collider. In such a case, bounds from the searches of long-lived multi-charged particles apply, which are approximately $m_{\chi_\ell} \gtrsim 800$ GeV [76, 77]. This translates into a bound on the vector mass of $M_L, M_E \gtrsim 850 - 970$ GeV, for Yukawa couplings of $y_L, y_E = 0.3 - 1$, leading to a stringent bound on the possible contribution to the $h \rightarrow \gamma\gamma$ rate once the stability of the vacuum is required. In particular, a 20% enhancement can be obtained only for $y_L, y_E \gtrsim 0.9$, with $M_L, M_E \gtrsim 950$ GeV, and the Higgs quartic runs negative at scales below ~ 10 TeV.

The previous bounds do not apply, if the new physics scale Λ is below 10^3 TeV. In this case, generic bounds from LFV processes imply some mild structure in the Wilson coefficients of dimension six operators. Depending on the flavor structure, the mass m_{χ_ℓ} , and the new physics scale, the lightest charge three state can decay either promptly or with a displaced vertex. Assuming prompt decay, from (53) one can see, that one order in magnitude in the new physics scale, $\Lambda \approx 10^2$ TeV translates to a mass limit of $m_{\chi_\ell} \gtrsim 125$ GeV. Even for such low masses, the UV completion of this model can occur at higher scales than those demanded from vacuum stability considerations in the $n = 0$ case [36]. Searches for many leptons [79, 80, 82] or leptons from displaced vertices [83] can in principle probe larger masses for the new leptons, but such searches could depend strongly on the flavor structure. In addition, present searches require in almost all cases large missing momentum and are therefore not applicable to our case. Since the new charge three leptons are pair produced with a cross-section of $\sim 100 - 0.1$ fb for masses of $m_{\chi_\ell} = 300 - 1000$ GeV at the $\sqrt{s} = 8$ TeV LHC, we expect that a dedicated analysis utilizing existing data could already constrain the parameter space of this model. In particular, a search for the striking signature of six leptons in the final state may lead to strong constraints on the vector fermion mass scale. A detailed study of the collider phenomenology in these scenarios will be presented elsewhere.

C. Decays of the Vector-Like Leptons: $n = 1$ Case

In the $n = 1$ scenario, the couplings of the vector-like leptons to SM matter allow for the direct decay of the lightest charge 2 state into a SM lepton and a W . The flavor observables discussed in Section IV constrain combinations of these couplings and are collected in the left column of Table I. The right column of Table I shows constraints on the individual Yukawa couplings from Z pole observables, which result in the bounds $y_{Le} \lesssim 0.01$ for electrons and $y_{L\mu}, y_{L\tau} \lesssim 0.1$ for muons and taus, assuming vector masses of the order of the Higgs vev. Apart from the strong bound on the product of the couplings of the new charge two leptons into electrons and muons from $\mu \rightarrow e$

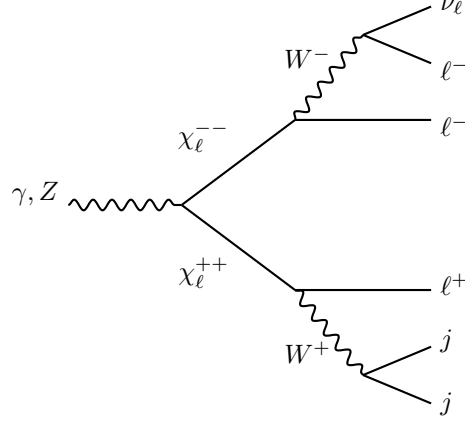


Figure 13. Decay chain of the doubly charged vector lepton in the $n = 1$ scenario.

conversion, flavor constraints are typically also satisfied in this parameter region.

The production and decay topology of the lightest charge two mass eigenstate in the $n = 1$ scenario is shown in Figure 13. The heavier charge two and charge one mass eigenstates dominantly decay into the lightest charge two mass eigenstate by radiating of W s and Z s, because the direct decay into SM matter is suppressed by the Yukawa couplings $y_{L\ell}$ and powers of the electro-weak over the vector mass scale. Since a sizable effect in $h \rightarrow \gamma\gamma$ prefers mass splittings of the order of the Higgs vev, it is safe to concentrate on the decays of the light charge two mass eigenstate. For simplicity, and because of flavor bounds, we will assume two scenarios, in which either only decays to muons or only decays to taus are allowed, with the respective other two mixing Yukawas set to zero,

$$\text{Only } \mu \text{ decays:} \quad y_{L\mu} = 0.1, \quad y_{Le} = y_{L\tau} = 0,$$

$$\text{Only } \tau \text{ decays:} \quad y_{L\tau} = 0.1, \quad y_{Le} = y_{L\mu} = 0.$$

In the first scenario, in which the new resonances couple directly only to muons, promising channels to probe the model are searches for multiple light leptons [79, 80]. The second scenario (only coupling to taus) can be probed by these searches as well in the case of leptonically decaying taus, but searches for hadronic taus and missing energy in the final state are in principle also sensitive to the new particles [81, 82, 84, 85]. We compare our signal cross section with the bounds from the most recent searches for three light leptons and missing energy [79]. In the case of hadronically decaying taus, we compute the bounds from searches for at least two hadronic taus of opposite sign and missing energy [81], same-sign dileptonic final states with at least one tau in the final state [84] as well as searches for two hadronic taus with no further requirement on the charges [85]. At last

Tri-boson	0.8 ± 0.8			
ZZ	0.25 ± 0.17	m_{χ_ℓ} [GeV]	N_{signal}^μ exp.	N_{signal}^τ exp.
$t\bar{t}V$	$0.21^{+0.30}_{-0.21}$	100	52.3	5.6
WZ	2.1 ± 1.6	200	82.5	15.6
SM reducible	1.0 ± 0.4	300	32.6	8.1
Σ SM	4.4 ± 1.8	400	12.1	3.6
Data	5	500	4.6	1.5
N_{signal} excl. (obs)	6.8			

Table II. Left: expected number of background events, observed number of events in the data and observed limit on the number of signal events (95% CL) for the relevant signal region, taken from the ATLAS search for three final state leptons with 20.7 fb^{-1} [79] (statistical and systematic errors are combined). Right: expected number of signal events after all cuts (see text for details) for the $n = 1$ scenario with $y_{L\mu} = 0.1$, $y_{L\tau} = y_{Le} = 0$ denoted by N_{signal}^μ as well as $y_{L\tau} = 0.1$, $y_{L\mu} = y_{Le} = 0$, denoted by N_{signal}^τ , for different masses of the lightest mass eigenstate.

we consider an ATLAS search for at least one hadronic tau and three light leptons [82].

In order to study the signal cross section, we implemented our model in FEYNRULES [87] and generated events using MADGRAPH 5 [88]. In the case of tau decays, PYTHIA-PGS was used for hadronization and detector simulation [89]. All cuts have been applied after the detector simulation. For the model parameters, $M = M_L = M_E$ and $y = y_L = y_E \in \mathbb{R}$ has been assumed. Fiducial tau efficiency tables for the ATLAS detector are publicly available, and we find that for the hard taus required in the searches considered here, the PGS simulation yields efficiencies roughly within 10% of the numbers listed in Table V in [86]. Since we are only interested in an estimate on the bound on the masses of the new resonances, we will not correct for these differences here.

1. Light Leptons in the Final State

The $n = 1$ scenario with couplings to light leptons leads to the same signature expected from the electro-weak production of charginos and neutralinos, which subsequently decay into three light leptons, neutrinos and the lightest neutralino (LSP). In the model presented here, there is no massive neutral final state, so that the strong exclusion bounds for a mass-less LSP apply. If the new resonances are assumed to couple only to taus, this final state will also be a promising channel in the case that the taus decay leptonically.

Several cuts have been imposed in [79], in order to reduce the background. Exactly three light

leptons are required. At least one pair of which must be of the same flavor with opposite charges (SFOS). In addition, the SFOS pair with an invariant mass closest to the Z mass must have an invariant mass of $m_{\text{SFOS}} < 81.2$ GeV or $m_{\text{SFOS}} > 101.2$ GeV (“ Z -veto”) in order to suppress ZZ background. The missing transverse energy is required to be more than $E_T^{\text{miss}} > 75$ GeV. An additional requirement on the transverse mass of the third lepton $m_T = \sqrt{2 E_T^{\text{miss}} p_T^\ell (1 - \cos \Delta\phi_{\ell, E_T^{\text{miss}}})}$ (the one which is not part of the Z pair) of $m_T > 110$ GeV is enforced in order to suppress background from WZ events. The third lepton is also required to have a transverse momentum of $p_T^\ell > 30$ GeV.

The background predictions after cuts, number of observed events and upper limit on contributions from new physics [79] are compiled on the left-hand side of Table II. We cross-checked our simulation by reproducing the irreducible ZZ background within its errors. The simulated number of signal events after cuts, depending on the mass of the lightest mass eigenstate of the model discussed here, is shown on the right-hand side of Table II. Since in our model a third lepton will always be the product of a W decay, in the low mass region $m_{\chi_\ell} < 200$ GeV, the E_T^{miss} cut is the most efficient cut on our signal, while the requirement on m_{SFOS} represents the strongest cut for higher masses. In the case of only direct couplings to muons, the limits on the mass of the lightest charge 2 mass eigenstate are roughly $m_{\chi_\ell} \gtrsim 460$ GeV. The scenario in which only direct couplings to taus are assumed allows for the weaker bound $m_{\chi_\ell} \gtrsim 320$ GeV.

2. Hadronic Taus in the Final State

In addition to the bound derived from the decay into light leptons, we considered three different searches for hadronic taus in the final state in order to further constrain the $n = 1$ scenario in which the doubly charged leptons only decay into taus and W s. We studied searches for opposite sign hadronic taus ($+ p_T^{\text{miss}}$) [81] or one hadronic tau together with a same-sign lepton ($+ \text{jets and } E_T^{\text{miss}}$) [84] in the final state, as well as searches for hadronic tau pairs, jets and large E_T^{miss} [85]. Finally, we consider an ATLAS search for three light leptons and one or more hadronic taus in the final state [82]. In all cases, we reproduced the diboson background and find reasonable agreement with the simulations done in the experimental studies.

In the ATLAS search for opposite sign hadronic taus and missing momentum [81], at least one opposite sign tau pair and no additional light leptons are required with transverse momenta $p_T^{\tau_1} > 40$ GeV and $p_T^{\tau_2} > 25$ GeV. A Z -veto on the invariant mass of each opposite sign tau pair is enforced, $m_{\tau\tau} > 91$ GeV or $m_{\tau\tau} < 71$ GeV, as well as a veto on all events with a b -jet in order to reject

background events from top quarks. In addition, the missing transverse energy needs to be larger than $E_T^{\text{miss}} > 40$ GeV and the largest value of $M_{T2}^2 = \min_{\not{p}_T = \not{p}_1 + \not{p}_2} \left[\max\{m_T^2(\not{p}_T^{\tau_1}, \not{p}_1), m_T^2(\not{p}_T^{\tau_2}, \not{p}_2)\} \right]$ computed among all opposite sign tau pairs needs to be larger than $M_{T2} > 100$ GeV in order to suppress W^+W^- background. This M_{T2} -cut turns out to reduce our signal the most. After all cuts, our signal cross section is below the experimental bound for the whole considered mass range ($m_{\chi_\ell} = 100 \dots 500$ GeV).

The CMS search [84] for two same sign leptons requires two jets and missing transverse energy. In order to reduce the high trigger rates, a significant bound on $E_T^{\text{miss}} > 120$ GeV and the scalar sum of jet transverse momenta $H_T = \sum p_T^{\text{jets}} > 450$ GeV has been set in the relevant search region. Transverse momentum cuts for all three lepton flavors, $p_T^e > 10$ GeV, $p_T^\mu > 5$ GeV and $p_T^\tau > 15$ GeV, and on each jet, $p_T^{\text{jet}} > 40$ GeV have been applied and a dilepton invariant mass of $m_{\ell\ell} > 8$ GeV has been required in order to suppress low-mass dilepton background. Events in which a third opposite-sign lepton is present and the invariant mass of any two opposite sign leptons lies within ± 15 GeV of the Z mass are vetoed. Our model signal cross section is strongly reduced by the stringent cuts on jet p_T s and missing energy, which can only result from the decay of one of the W s in our model, while the other W needs to provide the same sign lepton. As a result, the signal cross section stays below the experimental limit throughout the considered mass range.

A search for at least one hadronic tau pair in the final state and no further requirements on the charges has been done at ATLAS [85]. The aim of this search is primarily to constrain the gluino mass from decays through stau intermediate states. In the search region we considered, light leptons are vetoed, but at least two taus with $p_T^\tau > 20$ GeV are required. A cut on the sum of the transverse masses $m_T^{\tau_i} = \sqrt{2 E_T^{\text{miss}} p_T^{\tau_i} (1 - \cos \Delta\phi_{\tau_i, E_T^{\text{miss}}})}$ is set, $m_T^{\tau_1} + m_T^{\tau_2} \geq 150$ GeV, in order to suppress Z +jets events, and large $E_{\text{miss}}^T > 150$ GeV is required. At least two jets have to be present, with $p_T^{j_1} > 130$ GeV and $p_T^{j_2} > 30$ GeV, as well as a large scalar sum of the transverse momenta of these jets and taus $H_T = \sum p_T^{j_i} + \sum p_T^{\tau_i} > 900$ GeV. This H_T cut, the requirement for large missing energy as well as the cut on the sum of the transverse tau masses strongly reduce our signal cross section, so that the experimental bounds do not lead to constraints throughout the scanned mass range.

Finally, we consider a search from ATLAS for three light leptons and (at least) one hadronic tau in the final state [82]. In the scenario discussed here, this final state requires both W s to decay leptonically as well as one leptonic tau and one hadronic tau. In the considered search region an “extended Z -veto” has been employed, which means, that events with pairs, triplets or quadruplets of light leptons with an invariant mass within 10 GeV of $M_Z = 91.2$ GeV are vetoed. In addition,

ZZ	0.19 ± 0.05	m_{χ_ℓ} [GeV]	N_{signal}^τ exp.
ZWW	0.05 ± 0.05		
$t\bar{t}Z$	0.16 ± 0.12	100	9.3
Higgs	2.3 ± 0.06	200	23.1
SM reducible	1.4 ± 1.3	300	8.6
Σ SM	2.0 ± 1.3	400	3.4
Data	4	500	1.1
N_{signal} excl. (obs)	7.5		

Table III. Left: expected number of background events, observed number of events in the data and observed limit on the number of signal events (95% CL) for the relevant signal region, taken from the ATLAS search for three light leptons and at least one τ in the final state with 20.7 fb^{-1} [82] (statistical and systematic errors are combined). Right: expected number of signal events after all cuts (see text for details) for the $n = 1$ scenario with $y_{L\tau} = 0.1$, $y_{L\mu} = y_{Le} = 0$, denoted by N_{signal}^τ , for different masses of the lightest mass eigenstate.

selected events are required to either have missing energy of $E_{\text{miss}}^T > 100 \text{ GeV}$ or an effective mass $m_{\text{eff}} = E_{\text{miss}}^T + \sum p_T^{\text{e}_i} + \sum p_T^{\mu_i} + \sum p_T^{\tau_i} + \sum p_T^{\text{j}_i} > 400 \text{ GeV}$. These cuts are chosen in order to reduce the dominant backgrounds from ZZ , WZ and Z +jets. The signal cross section is reduced by the requirement to have exactly three light leptons and one hadronic tau, but not very sensitive on the additional cuts.

The background predictions after cuts, number of observed events and upper limit on contributions from new physics [82] are compiled on the left-hand side of Table III. On the right-hand side, the simulated number of signal events after cuts, depending on the mass of the lightest mass eigenstate of the model discussed here is shown. We estimate a bound on the mass of the lightest mass eigenstate of $m_{\chi_\ell} \gtrsim 310 \text{ GeV}$, which is very close to the value estimated based on the light lepton searches.

Thus, after considering both scenarios – decays of the new vector leptons only into one light lepton flavor or decays only into taus – we find bounds on the mass of the lightest mass eigenstate from the search for multiple light leptons in the final state, while searches for hadronic taus do not lead to further constraints on the mass of the resonances in the second scenario because of various tight cuts in the considered searches. For the scenario with direct couplings to muons we find an approximate mass bound of $m_{\chi_\ell} \gtrsim 460 \text{ GeV}$, while in the scenario in which only coupling to taus are assumed this mass is constrained to $m_{\chi_\ell} \gtrsim 320 \text{ GeV}$. This translates into bounds on the vector

mass of

$$m_{\chi_\ell} \gtrsim 460 \text{ GeV} \quad \Rightarrow \quad M_L, M_E \gtrsim 510 - 630 \text{ GeV}, \quad \text{for } y_L, y_E = 0.3 - 1, \quad (54)$$

$$m_{\chi_\ell} \gtrsim 320 \text{ GeV} \quad \Rightarrow \quad M_L, M_E \gtrsim 370 - 490 \text{ GeV}, \quad \text{for } y_L, y_E = 0.3 - 1. \quad (55)$$

In the tau case, these bounds imply that a 30% enhancement of the Higgs di-photon rate is possible with $y_E, y_L \gtrsim 0.7$, $M_L, M_E \gtrsim 440 \text{ GeV}$ and the Higgs quartic runs negative at a scale $\Lambda \lesssim 100 \text{ TeV}$. In the muon case instead, a 30% enhancement requires $y_E, y_L \gtrsim 1$, with $M_L, M_E \gtrsim 630 \text{ GeV}$ and the Higgs quartic runs negative already at a scale of a few TeV.

Finally, we want to mention, that a dedicated search based on existing data, looking for two hadronic W s and two light leptons in the final state might lead to stronger bounds on the parameter space.

3. Extended Scenario

The bounds in (54) and (55) can be relaxed by extending the model, such that the charge two leptons predominantly decay into a stable, neutral state with a mass close to the lightest charge two state. This can be arranged e.g. by adding to the model a SM singlet fermion χ_0 and coupling it to the hypercharge 2 singlet \tilde{E}_L and right-handed SM leptons $\ell_R^i = e_R, \mu_R, \tau_R$ via a dimension six operator

$$\mathcal{L} \supset \frac{c_{ij}}{\Lambda^2} (\bar{\chi}_0 \ell_R^i) (\tilde{E}_L \ell_R^j). \quad (56)$$

In order for the new decay mode of \tilde{E}_L to dominate over the decay into a W boson and SM lepton, the UV scale Λ where this operator is generated has to be sufficiently small, parametrically of order $\Lambda^4 \lesssim M^6/(v^2|y_{L\ell}|^2)$. For mixing Yukawas close to the bounds in Table I, this corresponds to scales around 10 TeV. The scale can be much higher if the mixing Yukawas are smaller. Note that the operator in (56) violates SM lepton number and generically also lepton flavor. As already mentioned in the $n = 2$ section, bounds on LFV dimension six operators, point to a new physics scale of $\Lambda > 10^3 \text{ TeV}$ [78]. If the operators in (56) arise at a much lower scale, the non observation of charged LFV calls for additional flavor structure in the corresponding Wilson coefficients.

If the spectrum is sufficiently compressed, searching for the lighter charge 2 state is very challenging and the constraints considered previously can be completely avoided. Searches for the heavier charge 2 state and the charge 1 state might be more promising in that case. Due to their larger masses and correspondingly smaller production cross sections, however, we expect that constraints

from current searches are still much weaker, compared to the minimal model. A detailed study of the collider phenomenology of the extended $n = 1$ scenario is left for future work. See also [90] for a very recent collider study of a related framework.

VII. CONCLUSIONS

In this work, we have analyzed an extension of the SM by one generation of new vector-like leptons with exotic hypercharges. We considered two models: One, in which the hypercharges of the new electro-weak doublets and singlets are given by $Y = Y_{\text{SM}} - n$, with $n = 1$ and Y_{SM} denoting the hypercharge of the SM leptons, and one in which $n = 2$. In both scenarios, sizable enhancements and suppressions of the $h \rightarrow \gamma\gamma$ decay rate are possible, depending on the relative sign of the Yukawa couplings of the new leptons. We did not consider scenarios with even higher hypercharges, $n \geq 3$, as in such cases the hypercharge gauge coupling will develop a Landau pole at very low scales $\lesssim 10^4$ TeV.

The bound on the scale at which one expects a UV completion due to vacuum instability considerations can in principle be relaxed considerably compared to a model in which the quantum numbers of the new leptons are copies of the SM leptons ($n = 0$). In the minimal $n = 1$ and $n = 2$ models, however, constraints from direct searches put strong bounds on the masses of the new leptons, which in turn constrain the possible modifications to $h \rightarrow \gamma\gamma$ as a function of their Yukawa couplings. In the $n = 2$ scenario, an enhancement of $R_{\gamma\gamma} \simeq 1.2$, for example, can be accommodated for new leptons of mass of order 800 GeV for a vector mass of $M = 950$ GeV and a UV scale of $\Lambda_{\text{UV}} \lesssim 10$ TeV. For $n = 1$, a 30% enhancement of $R_{\gamma\gamma}$ can occur for new leptons of mass of order 320 GeV for a vector mass of $M = 440$ GeV and a UV scale of $\Lambda_{\text{UV}} \lesssim 100$ TeV. In the widely discussed $n = 0$ scenario, instead, a 30% enhancement of $R_{\gamma\gamma}$ for a similar UV scale, $\Lambda_{\text{UV}} \lesssim 100$ TeV, would require new vector leptons as low as the Higgs mass with $M \simeq 250$ GeV, while slightly larger value of the new lepton masses, of order of the top quark mass, with vector masses $M \simeq 350$ GeV, would call for new bosonic degrees of freedom at the TeV scale.

Due to the exotic hypercharge assignments in the $n = 1$ and $n = 2$ cases, possible modifications of the $h \rightarrow Z\gamma$ rate can be larger compared to the $n = 0$ case. Still, we find that corrections to the $h \rightarrow Z\gamma$ rate typically do not exceed 10%. Precision measurements of the $h \rightarrow Z\gamma$ and $h \rightarrow \gamma\gamma$ rates can in principle distinguish between the considered cases, but it will be very challenging to achieve the required precision at the LHC.

We further discussed the new physics contributions to electric and magnetic dipole moments.

The non-standard hypercharge assignments strongly restrict the possible mixing operators with SM leptons, so that the leading contribution to the electron and quark EDMs only appear at 2-loop for both the $n = 1$ and $n = 2$ scenario. The corresponding Barr-Zee diagrams contain the $h \rightarrow \gamma\gamma$ loop as a sub-diagram, and a modification of $R_{\gamma\gamma}$ is therefore correlated with a 2-loop contribution to EDMs and MDMs. This correlation allows in principle to constrain the imaginary part (EDMs) and the real part (MDMs) of the Yukawa couplings between the new leptons and the Higgs using the very precise measurements of these observables. We find, that the single new phase entering the contributions to EDMs in our setups has to be below the order of 10% in regions of parameter space with visible modifications of the $h \rightarrow \gamma\gamma$ rate. It should be stressed that – barring cancellations – this implies that CP violation in $h \rightarrow \gamma\gamma$ and $h \rightarrow Z\gamma$ is constrained to be well below the 1% level. Similarly, EDMs constrain the possible signature of a pseudoscalar component of the Higgs detectable in the $h \rightarrow ZZ$ channel to be well below the 10^{-4} level. Bounds from MDMs turn out to be much weaker and do not constrain the interesting parameter space, given the current precision of the experimental results and the SM predictions.

In the $n = 1$ scenario, the allowed mixing of the vector-like leptons with SM leptons leads to modifications of the couplings of the Z boson to SM leptons. The mixing is therefore constrained both by Z pole observables and by flavor observables like $\mu \rightarrow e$ conversion in nuclei and $\ell \rightarrow 3\ell'$ decays. We have computed the most important of these bounds and find that the mixing of the vector-like leptons with SM leptons has to be generically small. In particular, the current bounds on $\mu \rightarrow e$ conversion strongly constrain a simultaneous mixing with electrons and muons. The planned Mu2e experiment can improve this bound by orders of magnitude.

Finally, we discussed the collider signals of the two models, that we already utilized to evaluate the possible modifications to $h \rightarrow \gamma\gamma$ and $h \rightarrow Z\gamma$. The dominant production cross section is the pair production of the lightest charge two (three) state in the case of $n = 1$ ($n = 2$). In the $n = 2$ scenario, the decay of the charge three state can only be mediated through higher dimensional operators. Possible dimension six operators violate the SM lepton number and generically also violate lepton flavor. If we assume that these operators are suppressed by a scale sufficiently high such that the new leptons are metastable at collider scales, bounds from searches for stable charged particles apply and the lightest mass eigenstate has to be heavier than about $m_{\chi_\ell} \gtrsim 800$ GeV. It is possible that this bound could be softened in a modified scenario, where the higher dimensional operators arise at scales low enough, such that the lightest charge three states decay promptly inside the detector. Further studies would be necessary to explore this scenario.

For $n = 1$, the pair produced charge two leptons can lead to final states with two or more

leptons and missing energy. We studied the leading production of the lightest charge two mass eigenstate and the subsequent decay into W s and SM leptons. We assume only couplings to one lepton family in order to avoid bounds from lepton flavor violation. If the new vector leptons couple only to muons we find that searches for multiple light leptons and missing energy in the final state constrain the mass of this lightest state to be heavier than about $m_{\chi_\ell} \gtrsim 460$ GeV. The same analysis for a scenario in which only couplings to taus are assumed yields a weaker bound of $m_{\chi_\ell} \gtrsim 320$ GeV. A search for one hadronic tau and three light leptons leads to very similar bounds for the scenario in which only tau couplings are present.

We also studied the possibility of hadronic tau pairs in the final state and conclude that the present searches are not sensitive to our model. Future multi-lepton searches at LHC 13 as well as dedicated searches for 2 leptons and 2 hadronic W s should offer excellent opportunities to probe the considered model.

We briefly considered a modified $n = 1$ model, where the charge two leptons predominantly decay into an additional stable, neutral state with a mass close to the lightest charge two state. In this case searches for the charge 2 lepton are more challenging and the current bounds get relaxed.

In summary, the bounds from direct searches on the new vector leptons in the various scenarios that we have considered, are crucial in constraining the possibility of modifications of the $h \rightarrow \gamma\gamma$ and $h \rightarrow Z\gamma$ rates. In the case of enhancement of the $h \rightarrow \gamma\gamma$ rate, the bounds on the new physics scale from the requirement of the stability of the Higgs potential are slightly less stringent than those obtained in the case of suppression of the $h \rightarrow \gamma\gamma$ rate. In general one can achieve 30% (10%) modifications of the $h \rightarrow \gamma\gamma$ ($h \rightarrow Z\gamma$) rate, due to the effects of vector-like fermions with non-standard hypercharges.

ACKNOWLEDGMENTS

We would like to thank Prateek Agrawal, Stefania Gori, Aurelio Juste, Matthias Neubert, Pedro Schwaller, Carlos Wagner, Lian Tao Wang, and Felix Yu for many useful discussions. We also thank David Straub for useful comments. Furthermore, we would like to thank Rupert Coy for bringing to our attention a mistake in the numerical results of Table I in an earlier version of this paper. We would like to thank KITP Santa Barbara for warm hospitality and support during completion of this work. KITP is supported in part by the National Science Foundation under Grant No. NSF PHY11-25915. Fermilab is operated by Fermi Research Alliance, LLC under Contract No. De-AC02-07CH11359 with the United States Department of Energy. One of us,

M.B., is acknowledging the support of the Alexander von Humboldt Foundation. The research of W.A. was supported in part by Perimeter Institute for Theoretical Physics. Research at Perimeter Institute is supported by the Government of Canada through Industry Canada and by the Province of Ontario through the Ministry of Economic Development & Innovation.

Appendix A: Loop Functions

The loop functions for the Higgs to diphoton decay read

$$A_1(x) = -2 - 3x - 3(2x - x^2)f(1/x) \xrightarrow{x \rightarrow \infty} -7, \quad (\text{A1})$$

$$A_{1/2}(x) = 2x + 2(x - x^2)f(1/x) \xrightarrow{x \rightarrow \infty} \frac{4}{3}, \quad (\text{A2})$$

$$\tilde{A}_{1/2}(x) = 2xf(1/x) \xrightarrow{x \rightarrow \infty} 2, \quad (\text{A3})$$

in which $f(x) = (\arcsin \sqrt{x})^2$ for $x < 1$, which is the case relevant for us.

The functions that enter the approximate expressions for the $h \rightarrow Z\gamma$ rate read

$$h_1(x) = -\frac{1 + 2x + 2x^2 + x^3}{(1-x)^3} - \frac{3x(1+x^2)\log x}{(1-x)^4} \xrightarrow{x \rightarrow 1} 0, \quad (\text{A4})$$

$$h_2(x) = -\frac{1 + 10x + x^2}{3(1-x)^3} - \frac{2x(1+x)\log x}{(1-x)^4} \xrightarrow{x \rightarrow 1} 0, \quad (\text{A5})$$

$$h_3(x) = -\frac{1 + 11x + 11x^2 + x^3}{(1-x)^3} - \frac{6x(1+x)^2\log x}{(1-x)^4} \xrightarrow{x \rightarrow 1} 0. \quad (\text{A6})$$

Barr-Zee diagrams lead to the following 2-loop functions in EDMs and MDMs

$$g(x) = \frac{x}{2} \int_0^1 \frac{dy}{y(1-y)-x} \log\left(\frac{y(1-y)}{x}\right) \xrightarrow{x \rightarrow \infty} \frac{1}{2} \log x, \quad (\text{A7})$$

$$f(x) = \frac{x}{2} \int_0^1 \frac{dy(1-2y(1-y))}{y(1-y)-x} \log\left(\frac{y(1-y)}{x}\right) \xrightarrow{x \rightarrow \infty} \frac{1}{3} \log x. \quad (\text{A8})$$

Appendix B: Couplings

In this appendix we give explicit expressions for couplings of the new lepton mass eigenstates with the Higgs as well as with gauge bosons. The expressions apply to both the $n = 1$ and the $n = 2$ case. However, in the $n = 2$ case, all mixing Yukawas $y_{L\ell}$ vanish and have to be set to 0 in the following expressions.

The mass matrix \mathcal{M}_E of the vector-like leptons E can be diagonalized by a bi-unitary transformation

$$Z_L \mathcal{M}_E Z_R^\dagger = \begin{pmatrix} m_1 & 0 \\ 0 & m_2 \end{pmatrix}, \quad (\text{B1})$$

with $m_1 < m_2$ real and positive. The most general parametrization of the Z_L , Z_R matrices reads

$$Z_L = \begin{pmatrix} c_L e^{i(\phi_L + \phi_{c_L})} & s_L e^{i(\phi_L + \phi_{s_L})} \\ -s_L e^{i(\phi_L - \phi_{s_L})} & c_L e^{i(\phi_L - \phi_{c_L})} \end{pmatrix}, \quad Z_R = \begin{pmatrix} c_R e^{i(\phi_R + \phi_{c_R})} & s_R e^{i(\phi_R + \phi_{s_R})} \\ -s_R e^{i(\phi_R - \phi_{s_R})} & c_R e^{i(\phi_R - \phi_{c_R})} \end{pmatrix}, \quad (\text{B2})$$

with $s_L^2 + c_L^2 = s_R^2 + c_R^2 = 1$. We then denote the left- and right-handed components of the mass eigenstates by

$$\chi_L = (P_L \chi_1, P_L \chi_2)^T = Z_L (E_L, \tilde{E}_L)^T, \quad \chi_R = (P_R \chi_1, P_R \chi_2)^T = Z_R (\tilde{E}_R, E_R)^T, \quad (\text{B3})$$

in which $P_{L,R} = \frac{1}{2}(1 \pm \gamma_5)$ are the chiral projection operators.

We collect the remaining vector-like lepton N together with the charged SM leptons into vectors

$$\eta_L = (P_L e, P_L \mu, P_L \tau, P_L N)^T, \quad \eta_R = (P_R e, P_R \mu, P_R \tau, P_R N)^T, \quad (\text{B4})$$

even though they can only mix in the $n = 1$ scenario.

We parametrize the interactions of χ and η with the Higgs and with gauge bosons in the following generic way

$$\begin{aligned} \Delta \mathcal{L} = & e Q_\chi A_\mu \bar{\chi} \gamma^\mu \chi + e Q_\eta A_\mu \bar{\eta} \gamma^\mu \eta \\ & + e Z_\mu \left(\bar{\chi}_L \gamma^\mu g_{Z\chi\chi}^L \chi_L + \bar{\chi}_R \gamma^\mu g_{Z\chi\chi}^R \chi_R + \bar{\eta}_L \gamma^\mu g_{Z\eta\eta}^L \eta_L + \bar{\eta}_R \gamma^\mu g_{Z\eta\eta}^R \eta_R \right) \\ & + \frac{g_2}{\sqrt{2}} W_\mu \left(\bar{\chi}_L \gamma^\mu g_{W\chi\eta}^L \eta_L + \bar{\chi}_R \gamma^\mu g_{W\chi\eta}^R \eta_R + \bar{\eta}_L \gamma^\mu g_{W\eta\nu}^L \nu_L + h.c. \right) \\ & + h \left(\bar{\chi}_L g_{h\chi\chi} \chi_R + \bar{\eta}_L g_{h\eta\eta} \eta_R + h.c. \right). \end{aligned} \quad (\text{B5})$$

In the couplings of the photons we have $Q_\eta = -1$ for $\eta = \ell$ and $Q_\eta = Q_N$ for $\eta = N$. For the Higgs couplings with the mass eigenstates χ we find the following expressions

$$\begin{aligned} g_{h\chi\chi} = & \frac{m_1}{v} \begin{pmatrix} s_R^2 c_L^2 + s_L^2 c_R^2 & c_R s_R (c_L^2 - s_L^2) e^{i(\phi_{c_R} + \phi_{s_R})} \\ s_L c_L (c_R^2 - s_R^2) e^{-i(\phi_{c_L} + \phi_{s_L})} & -2 s_L c_L s_R c_R e^{-i\phi} \end{pmatrix} \\ & + \frac{m_2}{v} \begin{pmatrix} -2 s_L c_L s_R c_R e^{i\phi} & -s_L c_L (c_R^2 - s_R^2) e^{i(\phi_{c_L} + \phi_{s_L})} \\ -c_R s_R (c_L^2 - s_L^2) e^{-i(\phi_{c_R} + \phi_{s_R})} & s_R^2 c_L^2 + s_L^2 c_R^2 \end{pmatrix}, \end{aligned} \quad (\text{B6})$$

For the Higgs couplings with η we expand in first order in v^2/M_L^2 and find

$$g_{h\eta\eta} = \begin{pmatrix} \frac{y_e}{\sqrt{2}} \left(1 - \frac{3}{2} |y_{Le}|^2 \frac{v^2}{M_L^2} \right) & -\frac{y_e y_{Le}^* y_{L\mu} v^2}{\sqrt{2} M_L^2} & -\frac{y_e y_{Le}^* y_{L\tau} v^2}{\sqrt{2} M_L^2} & \frac{y_e y_{Le}^* v}{\sqrt{2} M_L} \\ -\frac{y_\mu y_{L\mu}^* y_{Le} v^2}{\sqrt{2} M_L^2} & \frac{y_\mu}{\sqrt{2}} \left(1 - \frac{3}{2} |y_{L\mu}|^2 \frac{v^2}{M_L^2} \right) & -\frac{y_\mu y_{L\mu}^* y_{L\tau} v^2}{\sqrt{2} M_L^2} & \frac{y_\mu y_{L\mu}^* v}{\sqrt{2} M_L} \\ -\frac{y_\tau y_{L\tau}^* y_{Le} v^2}{\sqrt{2} M_L^2} & -\frac{y_\tau y_{L\tau}^* y_{L\mu} v^2}{\sqrt{2} M_L^2} & \frac{y_\tau}{\sqrt{2}} \left(1 - \frac{3}{2} |y_{L\tau}|^2 \frac{v^2}{M_L^2} \right) & \frac{y_\tau y_{L\tau}^* v}{\sqrt{2} M_L} \\ \frac{y_{Le}}{\sqrt{2}} \left(1 - \frac{1}{2} |y_{Le}|^2 \frac{v^2}{M_L^2} \right) & \frac{y_{L\mu}}{\sqrt{2}} \left(1 - \frac{1}{2} |y_{L\mu}|^2 \frac{v^2}{M_L^2} \right) & \frac{y_{L\tau}}{\sqrt{2}} \left(1 - \frac{1}{2} |y_{L\tau}|^2 \frac{v^2}{M_L^2} \right) & \sum_\ell |y_{L\ell}|^2 \frac{v}{\sqrt{2} M_L} \end{pmatrix}. \quad (\text{B7})$$

For the couplings of the Z boson with χ we find,

$$g_{Z\chi\chi}^L = \frac{s_W}{c_W} Q_\chi \mathbb{1} + \frac{1}{2s_W c_W} \begin{pmatrix} c_L^2 & -c_L s_L e^{i(\phi_{c_L} + \phi_{s_L})} \\ -c_L s_L e^{-i(\phi_{c_L} + \phi_{s_L})} & s_L^2 \end{pmatrix}, \quad (\text{B8})$$

$$g_{Z\chi\chi}^R = \frac{s_W}{c_W} Q_\chi \mathbb{1} + \frac{1}{2s_W c_W} \begin{pmatrix} c_R^2 & -c_R s_R e^{i(\phi_{c_R} + \phi_{s_R})} \\ -c_R s_R e^{-i(\phi_{c_R} + \phi_{s_R})} & s_R^2 \end{pmatrix}. \quad (\text{B9})$$

The couplings of the Z boson with η read

$$g_{Z\eta\eta}^L = \frac{s_W}{c_W} Q_\eta \mathbb{1} - \frac{1}{2s_W c_W} \begin{pmatrix} -1 & 0 & 0 & \frac{2y_e y_{L_e}^* v^2}{M_L^2} \\ 0 & -1 & 0 & \frac{2y_\mu y_{L_\mu}^* v^2}{M_L^2} \\ 0 & 0 & -1 & \frac{2y_\tau y_{L_\tau}^* v^2}{M_L^2} \\ \frac{2y_e y_{L_e} v^2}{M_L^2} & \frac{2y_\mu y_{L_\mu} v^2}{M_L^2} & \frac{2y_\tau y_{L_\tau} v^2}{M_L^2} & 1 \end{pmatrix}, \quad (\text{B10})$$

$$g_{Z\eta\eta}^R = \frac{s_W}{c_W} Q_\eta \mathbb{1} - \frac{1}{2s_W c_W} \begin{pmatrix} |y_{L_e}|^2 \frac{v^2}{M_L^2} & \frac{y_{L_e}^* y_{L_\mu} v^2}{M_L^2} & \frac{y_{L_e}^* y_{L_\tau} v^2}{M_L^2} & \frac{v y_{L_e}^*}{M_L} \\ \frac{y_{L_\mu}^* y_{L_e} v^2}{M_L^2} & |y_{L_\mu}|^2 \frac{v^2}{M_L^2} & \frac{y_{L_\mu}^* y_{L_\tau} v^2}{M_L^2} & \frac{v y_{L_\mu}^*}{M_L} \\ \frac{y_{L_\tau}^* y_{L_e} v^2}{M_L^2} & \frac{y_{L_\tau}^* y_{L_\mu} v^2}{M_L^2} & |y_{L_\tau}|^2 \frac{v^2}{M_L^2} & \frac{v y_{L_\tau}^*}{M_L} \\ \frac{v y_{L_e}}{M_L} & \frac{v y_{L_\mu}}{M_L} & \frac{v y_{L_\tau}}{M_L} & 1 - \sum_\ell |y_{N_\ell}|^2 \frac{v^2}{M_L^2} \end{pmatrix}. \quad (\text{B11})$$

In the case of the left-handed couplings, in principle also flavor changing couplings among the SM leptons are generated at the first order in v^2/M_L^2 . However, they are additionally suppressed by tiny factors $y_\ell y'_\ell$ and therefore completely irrelevant for all practical purposes, and set to 0 in (B10).

The couplings of the W boson with χ and η read,

$$g_{W\chi\eta}^L = \begin{pmatrix} c_L e^{i(\phi_{c_L} + \phi_L)} & 0 \\ 0 & -s_L e^{i(\phi_L - \phi_{s_L})} \end{pmatrix} \begin{pmatrix} y_e \frac{y_{L_e} v^2}{M_L^2} & y_\mu \frac{y_{L_\mu} v^2}{M_L^2} & y_\tau \frac{y_{L_\tau} v^2}{M_L^2} & -1 \\ y_e \frac{y_{L_e} v^2}{M_L^2} & y_\mu \frac{y_{L_\mu} v^2}{M_L^2} & y_\tau \frac{y_{L_\tau} v^2}{M_L^2} & 1 \end{pmatrix}, \quad (\text{B12})$$

$$g_{W\chi\eta}^R = \begin{pmatrix} c_R e^{i(\phi_{c_R} + \phi_R)} & 0 \\ 0 & -s_R e^{i(\phi_R - \phi_{s_R})} \end{pmatrix} \begin{pmatrix} \frac{y_{L_e} v}{M_L} & \frac{y_{L_\mu} v}{M_L} & \frac{y_{L_\tau} v}{M_L} & -1 + \frac{1}{2} \sum_\ell \frac{|y_{L_\ell}|^2 v^2}{M_L^2} \\ \frac{y_{L_e} v}{M_L} & \frac{y_{L_\mu} v}{M_L} & \frac{y_{L_\tau} v}{M_L} & -1 + \frac{1}{2} \sum_\ell \frac{|y_{L_\ell}|^2 v^2}{M_L^2} \end{pmatrix}. \quad (\text{B13})$$

Finally also W couplings between N and the SM neutrinos ν are induced

$$g_{WN\nu_\ell}^L = -y_\ell \frac{y_{L_\ell} v^2}{M_L^2}, \quad (\text{B14})$$

where we neglected neutrino mixing, which is irrelevant for our study.

- [2] S. Chatrchyan *et al.* [CMS Collaboration], Phys. Lett. B **716** (2012) 30 [arXiv:1207.7235 [hep-ex]].
- [3] G. Aad *et al.* [ATLAS Collaboration], Phys. Rev. Lett. **108**, 111803 (2012) [arXiv:1202.1414 [hep-ex]].
- [4] ATLAS Collaboration, ATLAS-CONF-2012-091.
- [5] S. Chatrchyan *et al.* [CMS Collaboration], Phys. Lett. B **710**, 403 (2012) [arXiv:1202.1487 [hep-ex]].
- [6] CMS Collaboration, CMS PAS HIG-12-015.
- [7] M. Carena, S. Gori, N. R. Shah and C. E. M. Wagner, JHEP **1203**, 014 (2012) [arXiv:1112.3336 [hep-ph]].
- [8] U. Ellwanger, JHEP **1203**, 044 (2012) [arXiv:1112.3548 [hep-ph]].
- [9] B. Batell, S. Gori and L. -T. Wang, JHEP **1206**, 172 (2012) [arXiv:1112.5180 [hep-ph]].
- [10] A. Arhrib, R. Benbrik, M. Chabab, G. Moultaka and L. Rahili, JHEP **1204**, 136 (2012) [arXiv:1112.5453 [hep-ph]].
- [11] A. Arhrib, R. Benbrik and N. Gaur, Phys. Rev. D **85**, 095021 (2012) [arXiv:1201.2644 [hep-ph]].
- [12] L. Wang and X. -F. Han, JHEP **1205**, 088 (2012) [arXiv:1203.4477 [hep-ph]].
- [13] A. G. Akeroyd and S. Moretti, Phys. Rev. D **86**, 035015 (2012) [arXiv:1206.0535 [hep-ph]].
- [14] M. Carena, I. Low and C. E. M. Wagner, JHEP **1208**, 060 (2012) [arXiv:1206.1082 [hep-ph]].
- [15] H. An, T. Liu and L. -T. Wang, Phys. Rev. D **86**, 075030 (2012) [arXiv:1207.2473 [hep-ph]].
- [16] A. Joglekar, P. Schwaller and C. E. M. Wagner, JHEP **1212**, 064 (2012) [arXiv:1207.4235 [hep-ph]].
- [17] N. Arkani-Hamed, K. Blum, R. T. D'Agnolo and J. Fan, JHEP **1301**, 149 (2013) [arXiv:1207.4482 [hep-ph]].
- [18] L. G. Almeida, E. Bertuzzo, P. A. N. Machado and R. Z. Funchal, JHEP **1211**, 085 (2012) [arXiv:1207.5254 [hep-ph]].
- [19] A. Delgado, G. Nardini and M. Quiros, Phys. Rev. D **86**, 115010 (2012) [arXiv:1207.6596 [hep-ph]].
- [20] J. Kearney, A. Pierce and N. Weiner, Phys. Rev. D **86**, 113005 (2012) [arXiv:1207.7062 [hep-ph]].
- [21] K. Schmidt-Hoberg and F. Staub, JHEP **1210**, 195 (2012) [arXiv:1208.1683 [hep-ph]].
- [22] H. Davoudiasl, H. -S. Lee and W. J. Marciano, Phys. Rev. D **86**, 095009 (2012) [arXiv:1208.2973 [hep-ph]].
- [23] D. McKeen, M. Pospelov and A. Ritz, Phys. Rev. D **86**, 113004 (2012) [arXiv:1208.4597 [hep-ph]].
- [24] L. Wang and X. -F. Han, Phys. Rev. D **87**, 015015 (2013) [arXiv:1209.0376 [hep-ph]].
- [25] E. Bertuzzo, P. A. N. Machado and R. Zukanovich Funchal, JHEP **1302**, 086 (2013) [arXiv:1209.6359 [hep-ph]].
- [26] B. Batell, S. Gori and L. -T. Wang, JHEP **1301**, 139 (2013) [arXiv:1209.6382 [hep-ph]].
- [27] W. Altmannshofer, S. Gori and G. D. Kribs, Phys. Rev. D **86**, 115009 (2012) [arXiv:1210.2465 [hep-ph]].
- [28] G. Moreau, Phys. Rev. D **87**, 015027 (2013) [arXiv:1210.3977 [hep-ph]].
- [29] B. Batell, S. Jung and H. M. Lee, JHEP **1301**, 135 (2013) [arXiv:1211.2449 [hep-ph]].
- [30] H. Davoudiasl, I. Lewis and E. Ponton, arXiv:1211.3449 [hep-ph].
- [31] J. Kopp, E. T. Neil, R. Primulando and J. Zupan, Phys. Dark. Univ. **2**, 22 (2013) [arXiv:1301.1683 [hep-ph]].

- [32] J. Fan and M. Reece, JHEP **1306**, 004 (2013) [arXiv:1301.2597 [hep-ph]].
- [33] P. S. Bhupal Dev, D. K. Ghosh, N. Okada and I. Saha, JHEP **1303**, 150 (2013) [Erratum-ibid. **1305**, 049 (2013)] [arXiv:1301.3453 [hep-ph]].
- [34] A. Carmona and F. Goertz, arXiv:1301.5856 [hep-ph].
- [35] W. -Z. Feng and P. Nath, Phys. Rev. D **87**, 075018 (2013) [arXiv:1303.0289 [hep-ph]].
- [36] A. Joglekar, P. Schwaller and C. E. M. Wagner, arXiv:1303.2969 [hep-ph].
- [37] N. Maru and N. Okada, Phys. Rev. D **87**, 095019 (2013) [arXiv:1303.5810 [hep-ph]].
- [38] ATLAS Collaboration, ATLAS-CONF-2013-012.
- [39] CMS Collaboration, CMS PAS HIG-13-001.
- [40] M. Reece, New J. Phys. **15**, 043003 (2013) [arXiv:1208.1765 [hep-ph]].
- [41] K. Ishiwata and M. B. Wise, arXiv:1307.1112 [hep-ph].
- [42] R. Dermisek and A. Raval, arXiv:1305.3522 [hep-ph].
- [43] B. A. Dobrescu, G. D. Kribs and A. Martin, Phys. Rev. D **85**, 074031 (2012) [arXiv:1112.2208 [hep-ph]].
- [44] K. Kumar, R. Vega-Morales and F. Yu, Phys. Rev. D **86**, 113002 (2012) [arXiv:1205.4244 [hep-ph]].
- [45] S. Dawson and E. Furlan, Phys. Rev. D **86**, 015021 (2012) [arXiv:1205.4733 [hep-ph]].
- [46] M. R. Buckley and D. Hooper, Phys. Rev. D **86**, 075008 (2012) [arXiv:1207.1445 [hep-ph]].
- [47] S. Fajfer, A. Greljo, J. F. Kamenik and I. Mustac, arXiv:1304.4219 [hep-ph].
- [48] S. K. Garg and C. S. Kim, arXiv:1305.4712 [hep-ph].
- [49] M. B. Voloshin, Phys. Rev. D **86**, 093016 (2012) [arXiv:1208.4303 [hep-ph]].
- [50] J. R. Ellis, M. K. Gaillard and D. V. Nanopoulos, Nucl. Phys. B **106**, 292 (1976).
- [51] M. A. Shifman, A. I. Vainshtein, M. B. Voloshin and V. I. Zakharov, Sov. J. Nucl. Phys. **30**, 711 (1979) [Yad. Fiz. **30**, 1368 (1979)].
- [52] S. Bethke, Eur. Phys. J. C **64**, 689 (2009) [arXiv:0908.1135 [hep-ph]].
- [53] [Tevatron Electroweak Working Group and CDF and D0 Collaborations], arXiv:1107.5255 [hep-ex].
- [54] G. Degrandi, S. Di Vita, J. Elias-Miro, J. R. Espinosa, G. F. Giudice, G. Isidori and A. Strumia, JHEP **1208**, 098 (2012) [arXiv:1205.6497 [hep-ph]].
- [55] D. Buttazzo, G. Degrandi, P. P. Giardino, G. F. Giudice, F. Sala, A. Salvio and A. Strumia, arXiv:1307.3536 [hep-ph].
- [56] M. E. Machacek and M. T. Vaughn, Nucl. Phys. B **222**, 83 (1983).
- [57] M. E. Machacek and M. T. Vaughn, Nucl. Phys. B **236**, 221 (1984).
- [58] M. E. Machacek and M. T. Vaughn, Nucl. Phys. B **249**, 70 (1985).
- [59] C. Ford, I. Jack and D. R. T. Jones, Nucl. Phys. B **387**, 373 (1992) [Erratum-ibid. B **504**, 551 (1997)] [hep-ph/0111190].
- [60] M. -x. Luo and Y. Xiao, Phys. Rev. Lett. **90**, 011601 (2003) [hep-ph/0207271].
- [61] A. Djouadi, V. Driesen, W. Hollik and A. Kraft, Eur. Phys. J. C **1**, 163 (1998) [hep-ph/9701342].
- [62] J. J. Hudson, D. M. Kara, I. J. Smallman, B. E. Sauer, M. R. Tarbutt and E. A. Hinds, Nature **473**, 493 (2011).

- [63] D. M. Kara, I. J. Smallman, J. J. Hudson, B. E. Sauer, M. R. Tarbutt and E. A. Hinds, *New J. Phys.* **14**, 103051 (2012) [arXiv:1208.4507 [physics.atom-ph]].
- [64] C. A. Baker, D. D. Doyle, P. Geltenbort, K. Green, M. G. D. van der Grinten, P. G. Harris, P. Iaydjiev and S. N. Ivanov *et al.*, *Phys. Rev. Lett.* **97**, 131801 (2006) [hep-ex/0602020].
- [65] W. C. Griffith, M. D. Swallows, T. H. Loftus, M. V. Romalis, B. R. Heckel and E. N. Fortson, *Phys. Rev. Lett.* **102**, 101601 (2009).
- [66] G. F. Giudice, P. Paradisi and M. Passera, *JHEP* **1211**, 113 (2012) [arXiv:1208.6583 [hep-ph]].
- [67] K. Kannike, M. Raidal, D. M. Straub and A. Strumia, *JHEP* **1202**, 106 (2012) [Erratum-ibid. **1210**, 136 (2012)] [arXiv:1111.2551 [hep-ph]].
- [68] M. Baak, M. Goebel, J. Haller, A. Hoecker, D. Kennedy, R. Kogler, K. Moenig and M. Schott *et al.*, *Eur. Phys. J. C* **72**, 2205 (2012) [arXiv:1209.2716 [hep-ph]].
- [69] L. Lavoura and J. P. Silva, *Phys. Rev. D* **47**, 2046 (1993).
- [70] S. Schael *et al.* [ALEPH and DELPHI and L3 and OPAL and SLD and LEP Electroweak Working Group and SLD Electroweak Group and SLD Heavy Flavour Group Collaborations], *Phys. Rept.* **427**, 257 (2006) [hep-ex/0509008].
- [71] R. Kitano, M. Koike and Y. Okada, *Phys. Rev. D* **66**, 096002 (2002) [Erratum-ibid. **D 76**, 059902 (2007)] [hep-ph/0203110].
- [72] J. Kaulard *et al.* [SINDRUM II Collaboration], *Phys. Lett. B* **422**, 334 (1998).
- [73] W. H. Bertl *et al.* [SINDRUM II Collaboration], *Eur. Phys. J. C* **47**, 337 (2006).
- [74] R. J. Abrams *et al.* [Mu2e Collaboration], arXiv:1211.7019 [physics.ins-det].
- [75] K. Hayasaka *et al.* [Belle Collaboration], *Phys. Lett. B* **687**, 139 (2010) [arXiv:1001.3221 [hep-ex]].
- [76] G. Aad *et al.* [ATLAS Collaboration], *Phys. Lett. B* **722**, 305 (2013) [arXiv:1301.5272 [hep-ex]].
- [77] S. Chatrchyan *et al.* [CMS Collaboration], arXiv:1305.0491 [hep-ex].
- [78] A. de Gouvea and P. Vogel, *Prog. Part. Nucl. Phys.* **71**, 75 (2013) [arXiv:1303.4097 [hep-ph]].
- [79] ATLAS Collaboration, ATLAS-CONF-2013-035.
- [80] CMS Collaboration, CMS-PAS-SUS-12-022.
- [81] ATLAS Collaboration, ATLAS-CONF-2013-028.
- [82] ATLAS Collaboration, ATLAS-CONF-2013-036.
- [83] S. Chatrchyan *et al.* [CMS Collaboration], *JHEP* **1302**, 085 (2013) [arXiv:1211.2472 [hep-ex]].
- [84] S. Chatrchyan *et al.* [CMS Collaboration], *Phys. Rev. Lett.* **109**, 071803 (2012) [arXiv:1205.6615 [hep-ex]].
- [85] ATLAS Collaboration, ATLAS-CONF-2013-026.
- [86] G. Aad *et al.* [ATLAS Collaboration], *Phys. Rev. D* **87**, 052002 (2013) [arXiv:1211.6312 [hep-ex]].
- [87] N. D. Christensen and C. Duhr, *Comput. Phys. Commun.* **180**, 1614 (2009) [arXiv:0806.4194 [hep-ph]].
- [88] J. Alwall, M. Herquet, F. Maltoni, O. Mattelaer and T. Stelzer, *JHEP* **1106**, 128 (2011) [arXiv:1106.0522 [hep-ph]].
- [89] T. Sjostrand, S. Mrenna and P. Z. Skands, *JHEP* **0605**, 026 (2006) [hep-ph/0603175].

- [90] A. Alloul, M. Frank, B. Fuks and M. R. de Traubenberg, arXiv:1307.1711 [hep-ph].